The influence of structural inheritance and multiphase extension on rift development, the northern North Sea

Thomas B. Phillips[1, 2]; Hamed Fazlikhani[2, †]; Rob L. Gawthorpe[2]; Haakon Fossen[2, 3]; Christopher A-L. Jackson[4]; Rebecca E. Bell[4]; Jan I. Faleide[5]; Atle Rotevatn[2]

[1] Department of Earth Sciences, Durham University, Science Labs, Elvet Hill, Durham, DH13LE

[2] Department of Earth Science, University of Bergen, PO Box 7800, 5020 Bergen, Norway

[3] Natural History Collections, University of Bergen, PO Box 7800, 5020 Bergen, Norway

[4]Basins Research Group (BRG), Department of Earth Science and Engineering, Imperial College, Prince Consort Road, London SW7 2BP, UK

[5] Department of Geosciences, University of Oslo, PO Box 1047, 0316 Oslo, Norway

[†]Present address: GeoZentrum Nordbayern, Friedrich-Alexander-Universität (FAU) Erlangen-Nürnberg, Schlossgartern 5, 91054 Erlangen, Germany

Key points

- The regional evolution of the northern North Sea rift is documented throughout late Permian-early Triassic and Late Jurassic-Early Cretaceous rift phases.
- Pre-existing structural heterogeneities may control the initial geometry of rift-related faults and associated syn-rift depocentres when favourably oriented and may also segment faults and depocentres
- Rift activity migrates throughout the evolution of the rift, showing a decreased influence from structural inheritance and increased localisation of rift activity during subsequent phases.

Abstract

The northern North Sea rift evolved through multiple rift phases within a highly heterogeneous crystalline basement. The geometry and evolution of syn-rift depocentres during this multiphase evolution, and the mechanisms and extent to which they were influenced by pre-existing structural heterogeneities remain elusive, particularly at the regional scale.

Using an extensive database of borehole-constrained 2D seismic reflection data, we examine how the physiography of the northern North Sea rift evolved throughout late Permian-Early Triassic (RP1) and Late Jurassic-Early Cretaceous (RP2) rift phases, and assess the influence of basement structures related to the Caledonian orogeny and subsequent Devonian extension. During RP1, the location of major depocentres, the Stord and East Shetland basins, was controlled by favorably oriented Devonian shear zones. RP2 shows a diminished influence from structural heterogeneities, activity localises along the Viking-Sogn graben system and the East Shetland Basin, with negligible activity in the Stord Basin and Horda Platform. The Utsira High and the Devonian Lomre Shear Zone form the eastern barrier to rift activity during RP2. Towards the end of RP2, rift activity migrated northwards as extension related to opening of the proto-North Atlantic becomes the dominant regional stress as rift activity in the northern North Sea decreases.

Through documenting the evolving syn-rift depocentres of the northern North Sea rift, we show how structural heterogeneities and prior rift phases influence regional rift physiography and kinematics, controlling the segmentation of depocentres, as well as the locations, styles and magnitude of fault activity and reactivation during subsequent events.

1 Introduction

Continental rifts often develop through multiple phases of extension within lithosphere containing structural heterogeneities inherited from earlier orogenic events. At the regional scale, faults in certain areas may be reactivated during later rift phases whilst others remain inactive, resulting in the migration of syn-rift depocentres and fault activity throughout the evolution of a rift. The evolution of this rift throughout multiple superposed tectonic events is also able to record the influence of any pre-existing structural heterogeneities within the lithosphere.

Pre-existing structures, along with early phases of rifting, can exert a considerable influence over the distribution of fault activity and the geometry and evolution of syn-rift depocentres during subsequent rift phases. Pervasive basement fabrics can directly control the geometry of faults and the (rift) basins they bound (e.g. Daly et al. 1989; Morley et al. 2004; Paton & Underhill 2004; Gontijo-Pascutti et al. 2010; Salomon et al. 2015; Phillips et al. 2016; Fazlikhani et al. 2017; Phillips et al. 2017; Skyttä et al. 2019; Vasconcelos et al. 2019). Discrete structures may also locally perturb the regional stress field, causing faults to strike oblique to the regional extension direction (Corti et al. 2007; Corti 2008; Morley 2010; Philippon et al. 2015; Morley 2017; Rotevatn et al. 2018; Samsu et al. 2019). In other instances, pre-rift basement structures may also retard lateral fault propagation and thus cause fault and rift segmentation (Koopmann et al. 2014; Fossen et al. 2016; Brune et al. 2017). Earlier phases of extension may also modify the crustal and lithospheric structure of rift systems. Faults related to earlier rift phases interact with, and may exhibit controls over the growth of newly formed normal faults (e.g. Bell et al. 2014; Nixon et al. 2014; Duffy et al. 2015; Henstra et al. 2015; Claringbould et al. 2017; Deng et al. 2017b; Morley 2017; Henstra et al. 2019); whilst, at the whole-rift scale, lithospheric thinning associated with earlier phases of extension may focus or dissipate strain during later rift phases (e.g. Odinsen et al. 2000; Cowie et al. 2005; Naliboff & Buiter 2015; Brune et al. 2017; Claringbould et al. 2017; Boone et al. 2018). Previous studies often focused on local (<10's of km) scale aspects of the influence of pre-existing structural heterogeneities on rift geometry and kinematics, with relatively few studies examining the regional, whole-rift (100's of km) scale (Daly et al. 1989; Corti 2009; Fazlikhani et al. 2017; Morley 2017). Furthermore, these studies often do not consider how structural inheritance is able to influence rift physiography throughout multiple rift phases, such as how they can influence fault reactivation and therefore the location and geometry of syn-rift depocentres during subsequent phases of rifting.

In this study, we focus on the northern North Sea rift located between the UK and Norway, which represents a failed rift marginal to the site of eventual North Atlantic breakup (e.g. Kristoffersen 1978; Dore et al. 1997; Roberts et al. 1999; Coward et al. 2003). The underlying crystalline basement of the rift is highly heterogeneous, containing numerous structures formed during the Caledonian orogeny and a subsequent period of Devonian extension (e.g. McClay et al. 1986; Andersen & Jamtveit 1990; Færseth et al. 1995; Reeve et al. 2013; Bird et al. 2014; Fossen et al. 2016; Phillips et al. 2016; Fazlikhani et al. 2017; Lenhart et al. 2019; Scisciani et al. 2019). The northern North Sea rift formed in response to two main phases of extension, initiating in the late Permian-Early Triassic (RP1) with a further phase in the Late Jurassic-Early Cretaceous (RP2) (e.g. Ziegler 1992; Færseth 1996; Coward et al. 2003).

Due to its long history of hydrocarbon exploration and production, the northern North Sea rift contains an abundance of geophysical and geological data, including near-complete coverage by 2D and 3D seismic reflection data and >6000 boreholes. This rich subsurface dataset has illuminated the tectono-stratigraphic evolution of the North Sea rift (e.g. Evans 2003), although, due to a previous relative scarcity of well and seismic data at deeper structural levels, a number of key questions regarding the early stages of rift evolution remain. Well data is typically collected at relatively shallow (2-3 km), more economic depths, with few wells penetrating deeper areas, particularly in the hangingwalls of major faults. Previously, imaging of basement structures was confined to regional seismic sections, often limited to 2D and at the expense of resolving shallow structure (BIRPS & ECORS 1986;

Klemperer & Hobbs 1991; Fossen et al. 2014; Gabrielsen et al. 2015). However, more recently basement structures have been resolved beneath the northern North Sea rift, particularly where they are situated at relatively shallow depths on the rift margins (Reeve et al. 2013; Bird et al. 2014; Phillips et al. 2016; Fazlikhani et al. 2017; Lenhart et al. 2019; Patruno et al. 2019).

Using key borehole-constrained stratigraphic horizons and intervening time-thickness maps covering the entire width of the northern North Sea rift (100,000 km^2), along with a detailed catalogue of the various basement structures (Fichler et al. 2011; Lundmark et al. 2013; Fossen et al. 2016; Fazlikhani et al. 2017), we characterise the structural style and depocentre geometry of the rift system throughout late Permian-Early Triassic and Late Jurassic-Early Cretaceous rift phases. The detailed catalog of basement structures also allows us to assess the influence of structural inheritance throughout multiphase evolution of the northern North Sea rift. We relate our findings to individual basin-scale studies in the northern North Sea and to other regional studies of rift systems elsewhere. The relatively well constrained basement structures beneath the northern North Sea rift (Færseth et al. 1995; Lundmark et al. 2013; Reeve et al. 2013; Phillips et al. 2016; Fazlikhani et al. 2017; Lenhart et al. 2019), in combination with the abundance of geophysical data imaging the deeper levels of the rift, make it the ideal natural laboratory in which to study how pre-existing structures and multiple phases of rifting influence the regional geometric and kinematic development of rift systems.

2 Regional setting and evolution of the North Sea

The northern North Sea rift, as referred to in this study, encompasses a ~250 x 450 km area (~100,000 km^2) between the East Shetland Platform and the western Norway coastline, and stretching from the along-strike continuation of the Møre-Trondelag Fault complex in the north to the E-W parallel with the southern tip of Norway (~58°N) in the south (Figure 1).

The crystalline basement beneath the northern North Sea rift is exposed onshore in Norway, the Shetland Islands and in northern Scotland. The basement initially formed during the Proterozoic Sveconorwegian orogeny (Roffeis & Corfu 2013; Slagstad et al. 2013), before being reworked during the Ordovician-Devonian Caledonian orogeny (Coward 1990; Milnes et al. 1997; McKerrow et al. 2000; Roberts 2003; Wiest et al. 2018). The Scandian phase of the Caledonian orogeny involved the collision of Baltica and Laurentia and the closure of the Iapetus Ocean (Gee et al. 2008), with the further collision of Avalonia to the south (McKerrow et al. 2000). Allocthonous nappes, including continental terranes from Baltica and Laurentia and oceanic terranes from the Iapetus Ocean (Hossack & Cooper 1986; Fossen & Dunlap 1998; Lundmark et al. 2013), were transported ESE on a décollement composed of mechanically weak Cambrian-Ordovician shales and phyllites, and emplaced onto the western margin of Baltica (Fossen & Rykkelid 1992; Milnes et al. 1997).

During the Lower Devonian, Caledonian thrusting was succeeded by E-W to NW-SE oriented extension, affecting an area stretching from onshore western Norway in the east to NE Scotland (Orcadian Basin) and Greenland in the west (McClay et al. 1986; Fossen 1992; Rey et al. 1997; Fossen 2010; Rotevatn et al. 2018). This extension was initially accommodated by extensional reactivation of the basal Caledonian thrust zone (Mode I extension of Fossen 1992), which accounted for around 30 km of extension across southern Norway. Subsequent extension was accommodated by the formation of km-scale shear zones that offset the entire Caledonian nappe sequence and which extend deep into the underlying crust (Mode II extension of Fossen 1992). Devonian shear zones and basins are identified onshore western Norway (Seranne & Seguret 1987; Fossen & Rykkelid 1992; Milnes et al. 1997; Vetti & Fossen 2012). These shear zones extend offshore beneath the northern North Sea rift and, along with additional structures that are not present onshore, are expressed in seismic reflection data as packages of coherent intra-basement reflectivity (e.g. Bird et al. 2014; Fossen et al. 2016; Phillips et al. 2016; Fazlikhani et al. 2017; Lenhart et al. 2019).

Following Devonian extension, the North Sea experienced further phases of extension and compression during the Palaeozoic and Mesozoic (Ziegler 1992; Coward et al. 2003). E-W oriented extension and associated magmatism occurred across Central Europe and the southern North Sea during the late Carboniferous-early Permian, mainly affecting the southern part of the study area (Figure 1) (Pegrum 1984; Wilson et al. 2004; Phillips et al. 2017). Post-rift thermal subsidence following late Carboniferous-early Permian extension led to the formation of the North and South Permian basins, and deposition of the evaporite-dominated Zechstein Supergroup, which influenced depocentre distribution in the southern section of the study area (Stewart & Coward 1995; Stewart et al. 2007; Jackson & Stewart 2017). The first major rift phase to have affected the northern North Sea rift initiated in the late Permian and continued into the Early Triassic (here termed Rift Phase 1; RP1) (Ziegler 1992; Coward 1995; Roberts et al. 1995; Færseth 1996; Coward et al. 2003). Extension associated with RP1 postdates the deposition of the Upper Permian Zechstein salt in the south of the area (Ziegler 1992; Jackson & Lewis 2013). The regional extension direction during RP1 is inferred to be E-W, based on the emplacement of N-S striking Permian-Triassic dykes onshore Norway (Fossen & Dunlap 1999), forming a dominantly N-S oriented rift (Ziegler 1992; Coward 1995; Roberts et al. 1995; Færseth 1996; Ter Voorde et al. 2000; Bell et al. 2014).

A period of relative tectonic quiescence followed RP1 (Ziegler 1992; Coward et al. 2003), although some faults remained active during this so-called ‘intra-rift’ period (Claringbould et al. 2017; Deng et al. 2017b). Early-Middle Jurassic thermal doming in the Central North Sea resulted in the erosion and removal of large thicknesses of strata across large parts of the North Sea (Underhill & Partington 1993; Davies et al. 1999; Quirie et al. 2018). The collapse of this thermal dome in the Middle to Late Jurassic was followed by a second rift phase (here termed Rift Phase 2; RP2), with activity lasting until the Early Cretaceous (Ziegler 1992; Underhill & Partington 1993; Færseth 1996; Færseth et al. 1997; Coward et al. 2003). Rift activity localized onto the ENE-WSW-striking Witch Ground Graben in the east, the NNW-SSE-striking Central Graben in the south, and the N-S-striking Viking Graben in the northern North Sea (Roberts et al. 1995; Færseth 1996; Odinsen et al. 2000; Ter Voorde et al. 2000; Davies et al. 2001; Coward et al. 2003).

However, the extension direction during RP2 across the northern North Sea is highly debated, with numerous studies stating that the extension direction was E-W similar to RP1 (Roberts et al. 1990; Bartholomew et al. 1993; Brun & Tron 1993; Bell et al. 2014), whereas others suggest that the extension direction rotated to NW-SE during RP2 (Færseth 1996; Færseth et al. 1997). During the latter stages and following RP2, the main area of extension migrated northwards to the Norwegian Sea and the opening of the proto-North Atlantic Ocean as the Artic and Atlantic rift systems to the north and west linked (Stewart et al. 1992; Ziegler 1992; Roberts et al. 1999). The offshore extension of the Møre-Trondelag Fault Zone (Figure 1) formed the boundary between the proto-North Atlantic and North Sea rifts (Dore et al. 1997).

3 Data and Methods

3.1 Data

This study uses a compilation of 29 2D seismic reflection surveys (~315,000 km total length) from the northern North Sea rift (Figure A1). These surveys display a range of orientations, were acquired over a range of time periods (1980-2012), and have different acquisition and processing parameters (see Table A1). Seismic line spacing is typically ~3 km (~6 km across parts of the East Shetland Basin), allowing the correlation of stratigraphic horizons and basement structures between individual lines. The majority of the sections used in this study are of a high quality and image down to ~9 s TWT, allowing us to constrain deeper structures and thus the early rift history. Stratigraphic horizons are tied to a large number of wells, of which 72 penetrate crystalline basement (Table A2) (Fazlikhani et al. 2017). Structural measurements were converted from the time to the depth domains using the velocity model of Fazlikhani et al. (2017), with those at deeper levels of the basin converted using interval velocities from Christiansson et al. (2000). Although parts of these surveys have been interpreted in local studies (e.g. Duffy et al. 2015; Claringbould et al. 2017; Deng et al. 2017b), this represents one of the first studies to integrate the available data with observations from these local studies to resolve the multiphase rift evolution of the whole of the northern North Sea.

3.2 Seismic interpretation

We map borehole-constrained stratigraphic horizons to describe the present-day rift geometry at different structural levels. These horizons represent i) the base of the late Permian-Early Triassic rift sequence (termed "Base RP1"), affected by both RP1 and RP2; ii) the base of the late Middle Jurassic-Early Cretaceous rift sequence (termed "Base RP2"), showing deformation solely related to RP2 and later activity; iii) the Base Cretaceous Unconformity, representing a prominent horizon within the upper RP2 interval (termed "Near Top-RP2"); and iv) a conservative "Post-rift" horizon corresponding to the top Cretaceous, unaffected by RP1 and RP2 activity.

Due to the large extent of these surfaces, and the potentially diachronous nature of rift activity across the rift, the mapped surfaces often correspond to different lithostratigraphic units in different areas and sub-basins (Figure 2). The Base RP1 surface typically corresponds to the base of the Triassic (i.e. base Smith Bank or Teist Formation; Figure 2), or younger strata where the Triassic is not present (i.e. structural highs or platform areas). One exception is that, where present, the Base RP1 horizon is represented by the base of the Zechstein Supergroup (Figure 2). Although this represents a Pre-RP1 interval, it forms a regionally prominent reflection and, in contrast to the Top Zechstein horizon (i.e. the base Triassic), does not include any short-wavelength relief associated with salt mobilization that would obscure our observations. The Base RP2 surface corresponds to the Middle Jurassic surface base Hugin and Sandnes formations in the south, and the base Heather Formation elsewhere. The Base Cretaceous Unconformity is typically taken to mark the syn- to post-RP2 transition across the northern

North Sea rift, although some RP2 fault activity postdates this horizon (Gabrielsen et al. 2001; Kyrkjebø et al. 2004; Bell et al. 2014). In the basin, this typically corresponds to the base Åsgard Formation (Figure 2), although it often merges with younger unconformities in shallower areas. The mapped Post-rift horizon is defined by the top Shetland Group across the entire northern North Sea rift (Figure 2).

The Base RP1 surface was mapped with moderate to high confidence across the Åsta Graben, Horda Platform, Stord Basin and East Shetland Basin due to an abundance of well control and its relatively shallow burial depth. Where it is situated at deeper levels beneath the axis of the northern North Sea rift, such as in the Viking and Sogn grabens, we are unable to accurately identify the exact reflection representing the Base RP1 horizon, although we can identify basin-bounding faults that extend through and offset the interval. Due to this 'corridor of uncertainty' beneath the North Viking and Sogn grabens, we are often unable to determine the true depth to the Base RP1 horizon, resulting in lower confidence in our interpretation of the depth and thickness of RP1 depocentres in these areas. The shallower horizons were mapped with high confidence across the rift.

We calculated time-thickness maps between our key stratigraphic surfaces to examine the multiphase evolution of the complete northern North Sea rift. The time-thickness map between the Base RP1 and Base RP2 defines syn-rift strata associated with RP1 (Figure 2). This map incorporates the relatively thin Pre-RP1 Zechstein Supergroup in the south as well as some RP1 post-rift strata (i.e. Late Triassic-Middle Jurassic) in the upper parts of the interval beneath the Base RP2 surface. Including these relatively thin packages of pre- and post-RP1 strata in the much thicker RP1 time-thickness map does not impact our ability to identify the various syn-rift depocentres, particularly as we also use seismic sections to identify wedge-shaped packages of growth strata that thicken into the hangingwalls of faults to confirm fault activity during each rift phase. The Base RP2 – Near Top-RP2 time-thickness map includes all Jurassic strata and records the majority of RP2 syn-rift strata. This is referred to as the "RP2" isochron. The Near Top-RP2 – Post-rift isochron incorporates any Late RP2 syn-rift strata and a significant post-rift interval that records the migration of activity from the North Sea to proto North Atlantic opening, and subsequent onset of post-rift thermal subsidence in the northern North Sea. This is referred to as the Late-syn- to Post-RP2 time thickness map.

4 Pre-existing structural framework of the northern North Sea

Based on seismic reflection transects and observations from previous studies, we establish the presence, orientations and geometry of pre-existing structural heterogeneities beneath the northern North Sea rift (Figure 3, 4), which we later compare to that of syn-rift depocentres during the evolution of the rift.

Crystalline basement has been penetrated by numerous wells across the northern North Sea and has been interpreted in terms of the tectonic units identified onshore in Norway and Scotland (Slagstad et al. 2011; Lundmark et al. 2013; Riber et al. 2015; Lenhart et al. 2019). The Utsira High, a long-lived, structural high in the centre of the northern North Sea rift has been shown to be underlain by dominantly granitic material, particularly in its southern part (e.g. wells 16/1-15, 16/5-1, 16/6-1; Figure 4) (Slagstad et al. 2011; Lundmark et al. 2013; Riber et al. 2015). Slagstad et al. (2011) and Lundmark et al. (2013) present U-Pb ages suggesting that the granitic basement of the Utsira High formed part of a volcanic arc incorporated into the Caledonian orogeny. This terrane may also be present beneath the East Shetland Basin and East Shetland Platform, and the Midland Valley Terrane onshore Scotland (Figure 1) (Fichler et al. 2011; Lundmark et al. 2013).

Mylonitic shear zones associated with the Caledonian orogeny and late syn- to post-Caledonian Devonian extension have been interpreted on seismic reflection data beneath the northern North Sea rift, where they are characterized by coherent packages of intrabasement reflectivity (Hurich & Kristoffersen 1988; Fossen & Hurich 2005; Reeve et al. 2013; Phillips et al. 2016; Fazlikhani et al.

2017). Here we briefly outline the general geometries of those shear zones referred to throughout this study (for a more detailed description of the shear zones, see Fazlikhani et al. 2017). In the northern part of the study area, the E-dipping Tampen Shear Zone strikes N-S beneath the eastern margin of the East Shetland Basin. Further west, the N-S to NE-SW-striking Ninian and Brent shear zones splay southwards away from the Tampen Shear Zone (Figure 3a, 4) (Fazlikhani et al. 2017). Along the eastern rift margin, W-plunging corrugations associated with the offshore Nordfjord-Sogn Detachment increase in dip towards the Sogn Graben (Lenhart et al. 2019) (Figure 4). Some of these corrugations appear spatially and perhaps kinematically linked with the E-W to NE-SW-striking Lomre Shear Zone (Figure 4) (Fazlikhani et al. 2017). The NE-SW-striking Hardangerfjord Shear Zone and the N-S-striking Øygarden Shear Zone lie in the footwall of the Øygarden Fault, with the Hardangerfjord Shear Zone also situated south of and in the footwall of the Øygarden Shear Zone (Figure 3b, 4). (Fazlikhani et al. 2017). Further south, the N-S- to NE-SW-striking Karmøy and Stavanger shear zones occur in the footwall of the Åsta Fault and beneath the Stavanger Platform respectively (Figures 3c, 4) (Thon 1980; Bøe et al. 2010; Phillips et al. 2016). The E-dipping Utsira Shear Zone tracks the western margin of the Stord Basin (Figure 3b, 4) (Fossen et al. 2016; Fazlikhani et al. 2017), and is represented by a series of shallowly E-dipping to sub-horizontal splays beneath the Utsira High (Figure 3c).

Reflections which may be related to the presence of deeply buried sediments can be identified beneath the Base RP1 surface (Figure 3). Coherent reflectivity beneath the Base RP1 surface across the Horda Platform may be related to Caledonian basement allochthons, as drilled by well 31/6-1 (Fossen et al. 2016), or in some areas may represent sedimentary strata (Figure 3a, 4). Further coherent reflectivity beneath the Base RP1 surface is identified beneath the East Shetland Platform which, based on well information, is interpreted as Devonian sedimentary strata (Figure 3b) (Patruno & Reid 2016; Patruno et al. 2019). Reflectivity beneath the Base RP1 surface in the Ling Depression is interpreted to correspond to sediments deposited during late Carboniferous-Permian extension, which affected only the southern margin of the study area, although some Devonian strata may also be present locally (Heeremans & Faleide 2004; Heeremans et al. 2004; Neumann et al. 2004; Jackson & Lewis 2016).

5 Present-day physiography of the northern North Sea rift

The Base RP1 surface records the cumulative effects of RP1 and RP2 basement-involved fault activity and defines a ~200 km wide, predominately N-S oriented rift, bordered by the East Shetland Platform to the west and the Norwegian mainland to the east (Figure 4). The western margin to the rift is here termed the Western Boundary Fault (Figures 3, 4), whereas the Øygarden and Åsta faults form the eastern rift margin south of the Måløy Slope (Figure 3c, 4). No rift-bounding fault is present across the Måløy Slope itself (Figure 4). The N-S- to NNE-SSW-striking Viking and Sogn grabens define the axis of the basin, with the Viking Graben comprising three segments, the South, Central and North (Figure 4).

In the northwest of the study area, the ~80 km wide East Shetland Basin contains numerous N-S- to NE-SW-striking, E- to SE-dipping normal faults. The depth to the Base RP1 surface in the East Shetland Basin ranges from 3-5 s TWT (~4-7 km) (Figure 3a, 4). To the north, the Base RP1 surface deepens to 6-7 s TWT (~11 km) across the NE-SW-striking Marulk and Magnus basins (Figure 4). East of the East Shetland Basin, the NNE-SSW-striking North Viking Graben reaches a depth of 6 s TWT (~9 km) along its western margin, and to the northeast, the N-S striking Sogn Graben reaches ~8 s TWT (~12 km) and may deepen further to the north (Figure 4). East of the North Viking and Sogn grabens, the Måløy Slope is characterized by relatively minor (~100 ms TWT (~200 m) throw) W- and E-dipping faults (Figure 4) (Færseth et al. 1995; Reeve et al. 2015; Lenhart et al. 2019).

The Horda Platform is located along the eastern margin of the northern North Sea rift, south of the Måløy Slope and Lomre Shear Zone and north of the Åsta Graben (Figure 4). This area encompasses the Stord Basin in the south and the Northern Horda Platform in the north. Its western margin is formed by the Oseberg Fault Block in the north and the Utsira High further south. The Brage Horst forms a N-S-striking high to the east of the Oseberg Fault Block (Figure 4). The Northern Horda Platform is dominated by the N-S-striking, W-dipping Tusse, Vette and Øygarden faults (Figure 4). Each of these faults displace the Base RP1 surface by ~1 s TWT (~1.5 km) (Whipp et al. 2014; Duffy et al. 2015) (Figure 3a). The depth to the Base RP1 surface across the Northern Horda Platform ranges from 3-4 s TWT (~4-7 km). The Vette Fault takes a prominent bend midway along its length where it strikes E-W and dips to the north. This area corresponds to a 'domain boundary' of Fossen et al. (2016) that correlates with the subcrop of the Lomre Shear Zone (Figure 4) (Fazlikhani et al. 2017).

The Utsira High represents a major intra-basin high where the Base RP1 surface is at ~1.8 s TWT (~3 km) depth. Northeast-dipping faults define the intra-high Augvald Graben (Olsen et al. 2017). East-dipping faults separate the Utsira High from the Stord Basin to the east (Figure 4), which, apart from the W-dipping Øygarden Fault along its eastern margin, is dominated by E-dipping faults (Figure 3b). The Øygarden Fault strikes N-S in the north, changing to NE-SW at the southern end of the Stord Basin. The E-dipping fault along the western margin of the Stord Basin margin generally strikes N-S, but changes to strike NE-SW in the north (Figure 4).

In the N-S- to NNE-SSW-striking Central segment of the Viking Graben, the Base RP1 surface reaches a maximum depth of ~7 s TWT (~11 km) and in the Southern segment of the Viking Graben it reaches depths of ~4 s TWT (~6 km). Along the eastern margin of the Viking Graben, the Beryl Embayment separates the Southern and Central segments (Figure 4).

In the southeast of the study area, the NE-SW-striking Ling Depression separates the Utsira and Sele highs. Further east, the Åsta Fault is separated from the Øygarden Fault by a ~60 km wide relay ramp (Figure 4). Zechstein Supergroup evaporites are also present across the south of the study area, thinning northwards in the South Viking and Åsta grabens, and thickening into the Ling Depression and Norwegian-Danish Basin. Halite-poor, and largely immobile parts of the evaporite sequence are present across the Utsira High, whereas a relatively thicker and halite-rich, and thus more mobile salt is present across the Sele High (Figure 3c) (Olsen et al. 2017; Sorento et al. 2018).

The present-day rift physiography at the Base RP2 and shallower depths differs to that of the Base RP1 surface. The physiography of the Near Top-RP2 (Base Cretaceous Unconformity; BCU) surface largely mirrors that of Base RP2, albeit at shallower depths. The rift displays an overall deepening to the north, with the Viking and Sogn grabens forming the dominant structural elements, and the Marulk and Magnus basins also representing prominent features (Figure 5a, b). Faults are expressed across the Northern Horda Platform (Figure 3a), but there are notably few faults expressed in the Stord Basin, which forms a ~80 km wide depression, and the Utsira High (Figure 3b, 5a, b). The South Viking Graben forms a narrow (~40 km wide) rift which begins to widen northwards along the western margin of the Oseberg Fault Block (Figure 5). Further north, Base RP2 and Near Top-RP2 surfaces describes a single wide rift from the East Shetland Basin to the Northern Horda Platform and Måløy Slope (Figure 5).

There is very little expression of faulting present across the Post-rift surface (Figure 3, 5c), with only the rift-bounding Western Boundary Fault expressed at this level. As at the Base RP2 and Near Top-RP2 surfaces, the rift forms a narrow depression (~55-60 km wide) across the South Viking Graben, which widens northwards to ~200 km across the East Shetland Basin and Måløy Slope (Figure 5c). In contrast to underlying surfaces, the deepest point of this surface (~2.6 s TWT; ~3 km) is located above the South Viking Graben rather than in the north (Figure 5c).

6 Rift Phase 1 - Late Permian-Early Triassic

Rift Phase 1 depocentres predominantly trend N-S to NE-SW, are located within the hangingwalls of N-S- to NE-SW-striking normal faults and are widely distributed across the northern North Sea rift (Figure 6). The width of the rift during RP1 is relatively uniform from north to south, with fault activity distributed across a 170 km wide zone from the East Shetland Basin to Northern Horda Platform in the north, and a 190 km wide zone from the South Viking Graben to the Åsta Graben in the south. However, in the south, fault activity is localised in the South Viking Graben and Stord Basin rift segments, separated by the relatively unfaulted Utsira High (Figure 6). RP1 strata are notably thin atop the Utsira High, although a ~250 ms (~400 m) thick interval is preserved within the NW-SE-striking Augvald Graben. A condensed succession of RP1 strata (100-400 ms TWT; 200-600 m) occurs across the Sele High. No RP1-related strata are preserved on platform areas outside of the main rift (Figure 6).

The main depocentres during RP1 were located in the Stord Basin and Northern Horda Platform along the eastern side of the rift (Figure 6, 7, 8), and the East Shetland Basin in the west (Figure 6, 9), each containing up to 3200 ms TWT (~4 km) of RP1 strata. Several internal depocentres were present in the Stord Basin, the largest of which, located within the hangingwall of the E-dipping fault along the western basin margin, which strikes N-S in the south and swings to trend NE-SW further north, paralleling the strike of the Utsira Shear Zone (Figure 6). In cross-section, the E-dipping faults within the Stord Basin appear to root downwards into the Utsira Shear zone (Figure 7). In a similar manner, the W-dipping Øygarden fault along the eastern margin of the Stord Basin soles onto the underlying Øygarden and Hardangerfjord shear zones (Figure 4, 7). A half-graben in the hangingwall of the Øygarden Fault displays clear syn-rift divergent wedges, confirming activity at this time (Figure 7). This N-S-striking depocentre (2000-2500 ms TWT; ~5 km thick) swings to strike NNE-SSW to the south where the fault strikes parallel to the Hardangerfjord Shear Zone (Figure 6, 7). To the southwest, along-strike of the Hardangerfjord Shear Zone, RP1 strata thicken into the bounding faults of the Ling Depression, which forms a NE-SW-striking graben depocentre containing 800 ms TWT (~1.4 km) of

RP1 strata (Figure 3c). To the east, the Åsta Graben also represents an RP1 depocentre containing ~700 ms TWT (~1.2 km) thick of RP1 strata (Figure 6).

North of the Stord Basin, a N-S-striking depocentre (up to ~2500 ms TWT; ~5 km thick) occurs in the hangingwall of an E-dipping fault southwest of the Vette Fault (Figure 6). Across the Northern Horda Platform, the Tusse, Vette and Øygarden faults form N-S-striking half graben depocentres containing divergent syn-rift wedges (Figure 6, 8). Further north, no RP1 strata are preserved on the Måløy Slope (Figure 6).

On the northeast side of the rift, the East Shetland Basin contains multiple depocentres (up to ~2500 ms TWT; ~5 km thick) in the hangingwalls of E-dipping faults (e.g. the Tern, Ninian and Brent faults), as well as the W-dipping Eider Fault (Figure 3a, 9). The geometry of these depocentres parallels the underlying Ninian, Brent and Tampen Spur shear zones, and the border faults to these depocentres also appear to merge together at depth, potentially linking with the underlying shear zones (Figures 6, 9) (Fazlikhani et al. 2017). North of the East Shetland Basin, the Marulk and Magnus Basins represent NE-SW-striking depocentres containing up to 2000 ms TWT (~5 km) of RP1 strata.

South of the East Shetland Basin, the Central and South Viking graben segments contain ~2000 ms TWT (~5 km) and ~1500 ms TWT (~3 km) of RP1 strata respectively. Rift Phase 1 activity appears subdued across the North Viking and Sogn Grabens (Figure 6). However, as we are unable to resolve the Base RP1 surface accurately in the data used in these areas, the magnitude of the RP1 depocentres is uncertain and our interpretation represents a minimum estimate of RP1 thickness (Figure 6). As a result, we cannot be certain that the observed depocentre beneath the Northern Horda Platform does not extend westwards and merge with that of the East Shetland Basin (Figure 6, 9). Observations from the East Shetland Basin suggest a regional thickening of Triassic strata towards the east, perhaps indicating that the depocentres may well merge beneath the North Viking Graben.

7 Rift Phase 2 – Late Jurassic-Early Cretaceous

The time-thickness map calculated for RP2, between the Base RP2 and Near Top RP2 surfaces, records the majority of syn-rift activity associated with Late Jurassic-Early Cretaceous rifting (Figure 3, 10). The distribution of fault activity during RP2 differed to that of RP1 (Figure 10). The most notable feature of the RP2 time-thickness map is that fault activity is focused along the Viking and Sogn grabens (Figure 10) and not in the Stord Basin and Northern Horda Platform (Figure 6). Rift activity in the south is localised along the ~25 km wide South Viking Graben, between the East Shetland Platform in the west and the Utsira High to the east (Figure 7). No RP2 activity is evident in the Stord Basin (Figure 7, 10). Rift activity widens northwards, with faults active across the Oseberg Fault Block and Brage Horst (Figure 10) (Færseth & Ravnås 1998). Further north, a ~700 ms TWT (~1.2 km) depocentre occurs in the hangingwall of the bend in the Vette Fault. In the north of the study area, fault activity was distributed over roughly the same area as in RP1 (~190 km), with activity widening in the east onto the Måløy Slope (Figures 3a, 10). The eastern boundary to the active rift during RP2 appears to follow the Utsira High in the south and the Lomre Shear Zone further north, with no activity observed east of this boundary (Figure 10).

The Viking Graben forms the main depocentre during RP2; individual depocentres, including the South, Central and Northern segments and the Sogn Graben, contain syn-rift divergent wedges, strike N-S and have a right stepping relationship to one another (Figure 3, 5). RP2 thicknesses reach 1350 ms TWT (~2.5 km) in the South Viking Graben and 1000 ms TWT (~2 km) in the Central Viking Graben, increasing to ~1800 ms TWT (~3.2 km) in the Sogn Graben (Figure 10). In the north, the NE-SW-striking Magnus Basin was a major depocentre during RP2, containing ~700 ms TWT (~1.2 km) of strata. RP1 faults within the East Shetland Basin were also reactivated during RP2. The Tern, Eider, Osprey, Brent and Murchison faults each contain RP2 syn-rift divergent wedges (up to ~500 ms TWT;

~1 km thick) in their hangingwalls (Figures 3a, 9) (Claringbould et al. 2017). The thickness of RP2 strata is reduced in certain areas of the East Shetland Basin, particularly in the immediate footwalls of faults, where RP2 strata are often absent due to erosion by the Base Cretaceous Unconformity (Figure 9).

Rift Phase 2 strata are mostly isopachous across the Northern Horda Platform (~400 ms TWT; 750 m thick) with no syn-rift divergent wedges observed in the hangingwalls of the Tusse, Vette and Øygarden Faults (Figure 8, 10). To the west, faults across the Oseberg Fault Block and along the eastern margin of the Brage Horst were active during RP2, with depocentres containing thicknesses of up to 500 ms TWT (~1 km) (Figure 3a, 10) (Færseth & Ravnås 1998). The ~800 ms TWT (~1.5 km) sedimentary thicknesses in the Stord Basin and Northern Horda Platform have a broad lobate planform geometry. The presence of clinoform sequences within these lobate intervals suggests that the lobate area represents the progradation of the Hardangerfjord and Sognefjord deltaic systems into accommodation space not generated through fault-controlled subsidence (Figure 3b, 7, 10) (Ravnås & Bondevik 1997; Ravnås et al. 2000; Dreyer et al. 2005; Sømme et al. 2013). South of the Hardangerfjord Delta, although a thickness change of ~200 ms TWT (~300 m) occurs across the Åsta Fault, no growth strata are present in the hangingwall, indicating a lack of tectonic activity on the Åsta Fault at this time (Figure 3c, 10). As with RP1, RP2 strata are thin across most of the Utsira High.

8 Late-syn-rift- to Post- Rift Phase 2 – Cretaceous

The late-syn-rift to post- RP2 time-thickness map (termed Late-syn- to Post-RP2), calculated between the Base Cretaceous Unconformity and the Post-rift surface, encompasses the entire Cretaceous interval and largely comprises a thick post-RP2 succession, although some relatively thin intervals of late RP2 syn-rift strata are present locally (Figure 9). A large, relatively isopachous unit typically forms the upper part of the Cretaceous interval, for example, across the East Shetland Basin and Sogn

Graben (Figures 9, 12), indicating widespread thermal subsidence in these areas post-RP2. Divergent stratal wedges are identified locally in the lower parts of the interval, indicating some syn-rift activity at this time (Figure 8, 9).

The distribution of depocentres across the Late-syn- to Post-RP2 time-thickness map is broadly similar to that recorded during RP2 (i.e. Base RP2 to Near Top-RP2) (Figure 11). The overall thickness of Late-syn- to Post-RP2 strata increases northwards, from ~950 ms TWT (~1.6 km) in the South Viking Graben to >3 s TWT (>5 km) in the Marulk and Magnus basins and the Sogn Graben (Figure 11). Late-syn- to Post-RP2 strata thin towards the south (<500 ms TWT; <800 m), with a thin interval present in the Stord Basin (Figure 7). The base of individual depocentres appear flatter than those identified in RP1 and RP2 and internally, the stratigraphy displays less pronounced thickening towards bounding faults (Figure 11). This indicates a lack of fault activity at this time and a predominance of post-rift thermal subsidence with, in some cases, the passive infilling of remnant relief related to earlier phases of rifting (Prosser 1993).

In the south, the South Viking Graben depocentre is bound to the east by the Utsira High, where Late-syn- to Post-RP2 strata are thin and locally absent (typically <150 ms TWT; <200 m) (Figures 10, 11). As in RP2, east of the Utsira High, no Late-syn- to Post-RP2 activity is recorded across the Stord Basin and Åsta Graben. Nevertheless, these areas contain 700-900 ms TWT (~1.2 km) of Late-syn- to Post-RP2 strata, likely deposited in accommodation related to post-RP1 thermal subsidence, as no RP2 activity occurred in this area (Figure 11). However, on the Northern Horda Platform, Late-syn- to Post-RP2 depocentres in the hangingwalls of the Tusse, Vette and Øygarden Faults contain up to ~600 ms TWT (~1 km) of Late-syn- to Post-RP2 strata. The majority of this strata forms divergent wedges (Figures 8, 11), indicating late-to-post RP2 reactivation of these faults (Bell et al. 2014). Late-syn- to Post-RP2 strata in the hangingwall of the Øygarden Fault are truncated by the overlying Base Cenozoic unconformity (equivalent to the Top Cretaceous) and therefore do not record the true depositional thickness (Figure 8).

Depocentres in the East Shetland Basin strike N-S in the south, swinging round to NE-SW further north (Figure 11). These depocentres contain 900-1300 ms TWT (1.6-2.3 km) of Late-syn- to Post-RP2 strata. These depocentres show limited thickening into the hangingwall of faults (with the Murchison Fault being an exception; Figure 9) and are typically characterized by sub-horizontal Cretaceous strata that onlap onto rotated Jurassic strata (Figure 9, 10), indicating a relative lack of fault activity in the East Shetland Basin at this time. We propose that these depocentres record passive filling of accommodation generated through Late Jurassic RP2 fault activity.

East of the East Shetland Basin, the Sogn Graben forms a large Late-syn- to Post-RP2 depocentre, containing over 3 s TWT (~5 km) of Cretaceous strata (Figure 11, 12). Syn-rift divergent wedges in the hangingwall of the eastern border fault of the Sogn Graben indicate that this structure was active during RP2 and the early stages of Late- Post RP2 (Figure 12). Faults along the western side of the Sogn Graben were active during RP2, but became inactive with their hangingwalls being passively filled during Late-syn- to Post-RP2. (Figure 12).

The generation of the accommodation for the upper post-rift strata in the Late-syn- to Post-RP2 interval appears to be related to thermal subsidence following RP2 activity (Figure 11), as evidenced by the large thicknesses present in the South and Central Viking grabens (Figure 3b, c). The thickness of Late-syn- to Post-RP2 strata is locally accentuated by fault activity in the Sogn Graben and Marulk and Magnus Basins, and local westerly tilting in the north of the study area (Figures 11, 12) (Brekke & Riis 1987). The increased thickness of Late-syn- to Post-RP2 strata in the north of the study area reflects a relative increase in activity related to proto-North Atlantic opening in the Møre Basin – Faroe-Shetland Basin – Rockall Trough axis to the north of the study area (Kristoffersen 1978; Roberts et al. 1999), which is related to a decrease in rift activity in the northern North Sea. The NE-SW-striking Marulk and Magnus Basins are aligned with the Atlantic rifts and Møre-Trondelag Fault Complex, reflecting this northwards migration of activity (Figure 11, 13) (Dore et al. 1997; Gabrielsen et al. 2001).

9 Discussion

We have explored the kinematic and geometric evolution of the northern North Sea rift throughout late Permian-Early Triassic (RP1) and Late Jurassic-Early Cretaceous (RP2) rift phases (Figure 13). Drawing on these observations, and those from other rift systems worldwide, we first discuss how pre-existing structures influence the initial rift physiography, before examining how the rift physiography and kinematics evolves during multiple phases of rifting.

9.1 Reactivation and inheritance of basement shear zones during rifting

Basement shear zones display a range of strikes beneath the northern North Sea rift (Figure 4). Numerical modelling, along with previous studies from the North Sea show that shear zones that strike within 45-90° of the regional extension direction, i.e. close to perpendicular, and have dips greater than 30° are able to influence fault strike during rifting. Rift-related faults often align in map view with shear zones displaying these characteristics (Bird et al. 2014; Phillips et al. 2016; Deng et al. 2017a; Fazlikhani et al. 2017). In the northern North Sea, the Åsta Fault strikes parallel to the offshore continuation of the Karmøy Shear Zone, whilst the Ling Depression parallels the offshore continuation of the Hardangerfjord Shear Zone (Fossen & Hurich 2005; Phillips et al. 2016; Fazlikhani et al. 2017). Similarly, the dominant N-S to NE-SW strike of faults in the East Shetland Basin parallels the underlying N-S- to NE-SW-striking Tampen, Brent and Ninian shear zones (Figure 4, 6, 13). However, in areas such as the Måløy Slope, shear zones strike sub-parallel to the interpreted E-W oriented regional stress field and are therefore oriented at high angles to rift-related faults, bearing little influence over their strike (Figure 13).

There are multiple geometric and kinematic interactions between basement shear zones and rift-related faults. Rift-related faults have previously been shown to exploit internal mylonitic layers within shear zones (Paton & Underhill 2004; Gontijo-Pascutti et al. 2010; Kirkpatrick et al. 2013; Salomon et al. 2015; Morley 2017; Heilman et al. 2019), with examples also documented from the northern North Sea rift (Figure 15) ('explotative' interaction of Phillips et al. 2016; Fazlikhani et al. 2017). Numerical and analog modelling has shown that rocks containing a fabric are weaker, and thus more likely to fail, along said fabric when subject to favorably oriented stress fields (Youash 1969; Zang & Stephansson 2009; Tong & Yin 2011; Chattopadhyay & Chakra 2013).

Basement shear zones in the northern North Sea may also locally perturb the regional stress field, causing nearby or newly-formed faults to locally align with the pre-existing structure rather than perpendicular to the extension direction ('merging' interaction of Phillips et al. 2016) (Figure 15). In the northern North Sea, the southern extension of the otherwise N-S-striking Øygarden Fault rotates to a NE-SW orientation and locally aligns with the NE-SW-striking Hardangerfjord Shear Zone, suggesting a local NE-SW-oriented stress field associated with the shear zone (Figure 6, 15). Similarly, faults defining the western margin of the Stord Basin follow the underlying Utsira Shear Zone in plan-view, rotating from N-S in the south to NE-SW further north. These faults merging with the shear zone at depth (Fazlikhani et al. 2017) (Figure 7). Instances where pre-existing heterogeneities locally perturbed the regional stress field have also been interpreted in the East African Rift (Corti et al. 2007; Philippon et al. 2015), the Gippsland Basin offshore Australia (Samsu et al. 2019), the Taranaki Basin offshore New Zealand (Collanega et al. 2018) and Thailand (Morley 2010, 2017). Although local faults may be misaligned with respect to the regional stress field, at the regional scale, overall rift kinematics do appear to be compatible with the extension direction (Corti et al. 2007; Philippon et al. 2015).

In contrast to the above interactions, where rift-related faults align with basement shear zones, E-W-striking shear zones oriented sub-parallel to the extension direction do not directly influence fault strike. However, these high-angle shear zones are often associated with areas of changing structural style and segmentation at both the fault and rift scales (Figure 15). At the fault-scale, these high-angle structures may form boundaries to the lateral propagation of faults (e.g. Nixon et al. 2014; Duffy et al. 2015), or may transfer strain from one fault to another within a rift (Bladon et al. 2015; Mortimer et al. 2016). In the northern North Sea, we identify similar interactions, where the Lomre Shear Zone correlates to a 90° bend along the Vette Fault (Figure 6) (Fossen et al. 2016; Fazlikhani et al. 2017; Lenhart et al. 2019), whilst the offshore corrugations of the Nordfjord-Sogn Detachment governing fault and rift architecture across the Måløy Slope (Lenhart et al. 2019).

At the rift-scale, shear zones oriented at high angles to the rift may segment rift basins and control the geometry and distribution of depocentres (see also 'Domain Boundaries' of Fossen et al. 2016). Within the northern North Sea this is particularly important for the distribution of major depocentres during RP1 and the segmentation of the Viking/Sogn graben system during RP2. The Tampen Shear Zone coincides with the boundary between the North and Central Viking Graben (Figure 10, 13a), whilst further north, Smethurst (2000) identifies two NW-SE-striking lineaments which bisect the North Viking and Sogn grabens. These structures oriented at high angles to the rift appear to constrain the length of each rift segment and thus segment the overall rift. Furthermore, the southern continuation of the Lomre Shear Zone projects between the South and Central Viking grabens and towards the Beryl Embayment (Figure 10, 13b). Potential mechanisms for this rift segmentation may include local stress perturbations surrounding the high-angle structures, as observed in the Turkana depression of the East African rift (Brune et al. 2017), or the inhibition or retardation of faults at these high-angle structures, as observed offshore West Greenland (Peace et al. 2017) and along the Atlantic rifted margins (Koopmann et al. 2014). Where they strike at 45-90° to the regional stress field, Devonian shear zones delineate the main depocentres during RP1. The Utsira and Hardangerfjord shear zones delineate the main Stord Basin depocentre (Figure 7, 13), whilst the Tampen, Brent and Ninian shear zones align with and delineate the main depocentres in the East Shetland Basin (Figure 9, 13). Areas underlain by high-angle shear zones (oriented 0-45°), such as the Viking Graben and Måløy Slope form less major depocentres during RP1, with the rift-related faults often constrained or segmented by the pre-existing structures (Figure 15). The presence of Devonian shear zones exerts a strong influence over the distribution and geometry of rift-related faults and therefore over depocentre geometry, at least during the initial stage of rifting (Figure 13, 16).

The Lomre Shear Zone appears to represent a key structure throughout the evolution of the northern North Sea, corresponding to the location of strain transfer during RP1 between the Stord Basin along the eastern rift margin and the East Shetland Basin further north along the western margin, and delineating the eastern boundary to rift activity in RP2 (Figure 13). This structure has an enhanced influence throughout the evolution of the rift compared to other interpreted Devonian shear zones. One possibility is that the Lomre Shear Zone extends to greater (i.e. mid-crustal) depths, or that it reactivates a Caledonian or earlier structure, both of which have been proposed for the Hardangerfjord Shear Zone further south, which also exerts a different influence over rift physiography (i.e. controlling the location and geometry of the rift-bounding faults in the Ling Depression (Fossen & Hurich 2005; Fossen et al. 2014; Gabrielsen et al. 2015). The Lomre Shear Zone has been proposed to represent the southern extension of the Nordfjord-Sogn Detachment by Færseth et al. (1995), although it does not appear to correlate with the structure onshore (Figure 4).

9.2 Strain localization around structural highs

The Utsira High forms a prominent intra-basin high within the northern North Sea, that appears only weakly faulted throughout RP1 and RP2 (Figure 4, 13). Multiple basement well penetrations across the Utsira High suggest that, at least in the upper parts of the crystalline basement, the high is granitic in origin (Slagstad et al. 2011; Lundmark et al. 2013; Riber et al. 2015; Fazlikhani et al. 2017). Granitic bodies typically have large density and rigidity contrasts with surrounding lithologies, and as such are often thought to resist extensional stresses and localise strain around their margins (Bott et al.

1958; Critchley 1984; de Castro et al. 2007; Howell et al. 2019). The North Pennine and Lake District batholiths in northern England (Critchley 1984; Chadwick et al. 1989; Evans et al. 1994; Kimbell et al. 2010; Howell et al. 2019), as well as granitic bodies interpreted beneath the North Sea (Donato & Tully 1982; Donato et al. 1983; Lundmark et al. 2013) typically form structural highs and appear relatively unaffected by major faulting. Furthermore, at larger scales, numerical modelling has demonstrated that deformation may localize around the margins of areas of stronger material (Pascal et al. 2002; Naliboff & Buiter 2015; Wenker & Beaumont 2016), as observed with the localization of rifting in orogenic belts surrounding cratonic areas (Daly et al. 1989; Ebinger et al. 1997). We suggest that the dominantly granitic nature of the Utsira High inhibits fault nucleation across the structure during RP1, with strain localised along its margins with the adjacent South Viking Graben and Stord Basin during RP1 and solely with the South Viking Graben during RP2 (Figure 13). Further north, where such granitic bodies are lacking, strain is more uniformly distributed, forming a single, wide rift (Figure 6, 13a).

9.3 Migration of rift activity during multiphase rifting

Rift physiography evolves during the multiphase evolution of the northern North Sea rift. Activity during RP1 is distributed over a wide area, forming a relatively uniform rift. Based on the position of the main depocentres, the main locus of rift activity passes through the Stord Basin and Northern Horda Platform along the eastern side of the rift, before switching to the western side at the Lomre Shear Zone and continuing northwards through the East Shetland Basin (Figure 13).

During RP2, the location and magnitude of the major depocentres bears less correlation to the location of Devonian shear zones and rift activity instead localises along the Viking and Sogn grabens, suggesting a decreasing influence from structural inheritance in controlling fault and depocentre geometry during RP2 (Figure 13). This diminishing influence of discrete basement structures may reflect an increasing thermal influence associated with the evolving thermal and rheological structure of the lithosphere. Progressive thinning of the lithosphere during extension is often associated with a narrowing of the overall rift system as upwelling asthenosphere is increasingly focused into a narrower area. The increasing thermal effects following lithospheric thinning may cause new rift-related faults to largely ignore pre-existing structural heterogeneities (Roberts et al. 1995; Odinsen et al. 2000; Cowie et al. 2005; Paton et al. 2016; Ragon et al. 2018). However, numerical modelling has also shown that, during multiphase rifting, the lithosphere beneath older rifts may strengthen during inter-rift periods and therefore be less prone to reactivation during later events (Naliboff & Buiter 2015). Within the northern North Sea, we observe an overall localization of the rift system from RP1 to RP2, suggesting that there may not have been sufficient time between rift phases to sufficiently strengthen the lithosphere, or that extension was more protracted throughout RP1 and RP2. However, strengthening of the lithosphere beneath the RP1 axis beneath the Stord Basin may also have contributed to the lack of activity in this area during RP2 and the localization of activity in the adjacent South Viking Graben (Figure 14). Observations from the East Shetland Basin and Oseberg Fault Block indicate that fault activity may continue, albeit at a reduced rate, in the inter-rift period between RP1 and RP2 (Claringbould et al. 2017; Deng et al. 2017b).

During its latter stages, and following RP2, tectonic activity migrated northwards to the NE-SW trending Marulk and Magnus basins and the Sogn Graben, with little fault activity observed elsewhere (Figure 11, 13). In addition, faults across the Northern Horda Platform that were not active during RP2, are active during Late-syn- to Post-RP2 (Figure 11). These faults were diachronously reactivated from west to east, with those in the west (i.e. towards the Oseberg Fault Block) potentially being active in the Late Jurassic (Bell et al. 2014). At this time, rift activity within the northern North Sea lessens and extension in the proto-North Atlantic to the north increases, resulting in a migration of rift activity northwards and an increase in fault activity in the north of the northern North Sea rift (i.e.

Marulk and Magnus Basins, Sogn Graben) (Kristoffersen 1978; Roberts et al. 1999; Coward et al. 2003).

Faults across the Northern Horda Platform are also reactivated during Late-syn- to Post-RP2, although this does not appear to be related to proto-North Atlantic extension as it is further north. Rather, Late-syn- to Post-RP2 reactivation of faults across the Northern Horda Platform is proposed to be related to flexural downbending occurring in response to the increase in tectonic activity to the north (Brekke & Riis 1987; Bell et al. 2014). This suggests that activity across the Northern Horda Platform during Late-syn- to Post-RP2 was mainly related to local flexural stresses and that the eastern margin of the rift (east of the Lomre Shear Zone and Utsira High) was only indirectly influenced by, and largely remained isolated from regional stresses post-RP1.

Although more localised during RP2, rift activity in the north of the study area occurs over roughly the same area in RP1 and RP2. However, in the south, rifting is localised in the South Viking Graben and Stord Basin during RP1 and solely the South Viking Graben during RP2, with little activity across the intervening Utsira High (Figure 14). Extension during RP2 was thought to be at least partly driven by stresses originating from the triple point of the trilete rift system of the Central, Witch Ground and Viking grabens (Rattey & Hayward 1993; Underhill & Partington 1993; Coward et al. 2003; Quirie et al. 2018). Based on it its relative proximity to the origin of this activity, and the potential for post-RP1 lithospheric strengthening beneath the Stord Basin (Naliboff & Buiter 2015), we suggest that upwelling asthenosphere associated with RP2 would be channeled beneath the South Viking Graben and buttressed by the Utsira High and Lomre Shear Zone to the east, resulting in the Stord Basin and Northern Horda Platform remaining inactive during RP2 (Figure 14).

9.4 Fault interactions during multiphase rifting

Based on the geometry and distribution of syn-rift depocentres, we observe that the N-S-striking faults across the Northern Horda Platform were active in RP1, inactive during RP2 and later reactivated during Late-syn- to Post-RP2 (Figures 6, 11, 13). This RP2 inactivity and Late-syn- to Post-RP2 reactivation contrasts with observations across East Shetland Platform, where fault activity is recorded during RP2 before reducing in Late-syn- to Post-RP2. This reactivation of faults across the Northern Horda Platform is associated with the formation of NW-SE-striking faults between the main N-S-striking faults, although these are not resolved in this study (Whipp et al. 2014; Duffy et al. 2015). These NW-SE-striking faults do not match with the proposed E-W to NW-SW oriented extension directions proposed for RP2 and are instead proposed to be related to local stress perturbations surrounding the larger N-S striking faults (Whipp et al. 2014; Duffy et al. 2015; Reeve et al. 2015), showcasing a similar mechanism to that observed between the shear zones and rift-related faults during RP1 (Figure 15).

In the East Shetland Basin, optimally-aligned (i.e. N-S-striking) RP1 faults were often not reactivated during RP2 (Tomasso et al. 2008; Claringbould et al. 2017). RP2 extension across the East Shetland Platform was largely accommodated by the formation of new, mostly E-dipping faults that cross-cut the pre-existing structures (Figure 9). Claringbould et al. (2017) propose that the lack of reactivation may reflect the increasing influence of thermal effects arising from previously thinned lithosphere, with the rift narrowing process causing incipient faults to preferentially dip towards the rift axis (Cowie et al. 2005; Claringbould et al. 2017). A similar process occurs in the East African rift, strain is initially accommodated over a wide area under the influence of pre-existing structures, before becoming localised towards the rift axis and neglecting the presence of any pre-existing structures (Corti 2009; Ragon et al. 2018).

10 Conclusions

In this study we document the regional-scale evolution of the North Sea throughout late Permian-Early Triassic and Late Jurassic-Early Cretaceous phases of extension. We evaluate how syn-rift depocentres and their associated normal faults evolve throughout multiple phases of rifting and assess the impact of structural inheritance.

Through documenting the regional-scale multiphase evolution of the northern North Sea rift, and comparing it to the detailed catalog of pre-existing structural heterogeneities beneath the rift, we show that:

1. Rift geometry and activity was highly spatially and temporally variable across the northern North Sea during late Permian-Early Triassic (RP1) and Late Jurassic-Early Cretaceous (RP2) rift events.
2. Extension occurred over a ~200 km wide area during RP1, from the East Shetland Basin to the Northern Horda Platform in the north and from the South Viking Graben to the Stord Basin in the south. The location of major depocentres during RP1 appears to have been heavily influenced by the presence of Devonian basement shear zones, the Utsira Shear zone and Øygarden/Hardangerfjord Shear zones align with the bounding faults of the Stord Basin, whilst faults in the East Shetland Basin mirror the geometry and dip direction of the underlying Tampen, Brent and Ninian shear zones.
3. Strain is transferred from the Stord Basin/Northern Horda Platform along the eastern margin of the rift in the south, to the East Shetland Basin along the western rift margin further north. The site of this strain transfer corresponds to the Lomre Shear Zone.
4. Rift-related faults may reactivate or align along pre-existing structures such as the Devonian shear zones either due to the reactivation of internal anisotropies or due to local stress perturbations around the structure In addition, shear zones situated at high angles to the regional stress field may be responsible for the segmentation of individual faults and rift basins, including the Viking Graben.

5. Rift activity localises onto the Viking and Sogn grabens during RP2, with negligible reactivation of structures along the eastern rift margin, i.e. the Stord Basin and Northern Horda Platform and activity along structures in the East Shetland Basin. The eastern margin of activity during RP2 is delineated by the Utsira High in the south and the Lomre Shear zone further north.
6. As extension in the northern North Sea wanes during the latter stages of RP2, rift activity migrates northwards towards the Sogn Graben and the Marulk and Magnus Basins. This migration of rift activity reflects extension related to the opening of the North Atlantic Ocean becoming the dominant regional stress. Increased rift activity in the north of the study area drives the local flexural reactivation of faults across the Northern Horda Platform.
7. The Utsira High represents a long-lived structural high that resists extension throughout RP1 and RP2.Following RP1, we propose that increased lithospheric thickness was preserved beneath the Utsira High with thinned lithosphere beneath the Stord Basin and South Viking Graben. As a result, we suggest that activity during RP2 was focused beneath the South Viking Graben and pinned eastwards at the Utsira High and Lomre Shear zone, causing the Stord Basin and Northern Horda Platform to the east to largely remain inactive.
8. The influence of pre-existing structural heterogeneities, here represented primarily by Devonian shear zones, exert a diminished influence over rift physiography during later rift phases. Although they delineate the boundary to activity during RP2, they do not control the main depocentres. The Viking Graben instead appears to be more influenced by modification of the lithospheric structure associated with the earlier phase of rifting.

We highlight how structural inheritance and multiple phases of rifting influence the regional geometry and evolution of rift systems. Pre-existing structural heterogeneities that are relatively well-aligned with the rift dictate the initial geometry of major rift-related faults and their associated syn-rift depocentres, whilst those oriented at relatively high-angles to the rift may segment faults and rifts. Furthermore, we show how rift activity migrates and localises across the rift during multiple phases of rifting, showing a decreased influence from structural inheritance and an increased role from thermal effects associated with prior phases of lithospheric thinning. However, pre-existing structures still exert some control over rift physiography and kinematics during these later events, determining the areas of rift activity, whether and which faults will be reactivated.

Figure captions

Figure 1 – Regional setting of the North Sea between the UK and Norway. The northern North Sea rift (NNS) study area is shown by the red rectangle. The locations of major lineaments identified onshore and offshore are marked by thick black lines after Fazlikhani et al. (2017). Onshore Norway basement geology from Fossen et al. (2016); grey areas correspond to Caledonian nappes, beige colors represent Proterozoic-aged basement whilst yellow colors indicate Devonian basins. The main offshore rift axes are shown in orange. MTFC – Møre-Trondelag Fault Complex; WGR – Western Gneiss Region; NSDZ – Nordfjord-Sogn Detachment Zone; BASZ – Bergen Arc Shear Zone; HSZ – Hardangerfjord Shear Zone; KSZ – Karmøy Shear Zone; SSZ – Stavanger Shear Zone; STZ – Sorgenfrei-Tornquist Zone.

Figure 2 – Regional stratigraphic columns across various sub-basins of the northern North Sea rift, showing the different lithostratigraphic units that comprise temporally consistent surfaces referred to and mapped throughout this study. Compiled from Patruno & Reid (2016) and NPD (2014).

Figure 3– Regional seismic sections across the northern North Sea rift from north to south. See Figure 1 for section locations and see appendix for uninterpreted sections. A) Interpreted seismic section stretching from the East Shetland Basin in the east to the Northern Horda Platform in the west. Key surfaces and structures referred to in this study are identified. B) Interpreted seismic section across the

central portion of the rift, from the Central Viking Graben to the Stord Basin. Note the presence of Devonian basins beneath the pre-rift surface on the East Shetland Platform and the identification of the Utsira Shear zone and the Hardangerfjord and Øygarden shear zones beneath the northern Utsira High and Stord Basin respectively. C) Interpreted seismic section across the southern portion of the rift, stretching from the South Viking Graben to the Åsta Graben and Stavanger Platform. Pre-rift strata of Carboniferous-Permian age are identified beneath the Ling Depression, Sele High and Åsta Graben, with the Utsira and Karmøy shear zones present beneath the Utsira High and Åsta Graben/Stavanger Platform respectively. Note that the Utsira High forms a series of sub-horizontal to E-dipping strands in this area. Data courtesy of TGS (A - NSR06-31182.0009614; B - NSR06-31154.0015823; C - NSR05-211321.0015647).

Figure 4 – Two-way-time structure map of the Base RP1 structure map, modified after Fazlikhani et al. (2017). See Figures 2 and 3 for structural level. The offshore extensions of Devonian shear zones are shown by white translucent lines (after Fazlikhani et al. 2017), with those referred to in the study labelled in grey. The Utsira High forms an intra-basinal high in the south of the area. The pink line represents the limit of mobile salt of the Zechstein Supergroup. Major structural lows include the Stord Basin, East Shetland Basin and the Viking Graben and Sogn Graben. Faults: WBF – Western Boundary Fault; ØF (S/C/N) – Øygarden Fault (South/Central/North); ÅF – Åsta Fault. Shear Zones: NSZ – Ninian Shear Zone; BSZ - Brent Shear Zone; TSZ – Tampen Shear Zone; LSZ – Lomre Shear Zone; USZ – Utsira Shear Zone; HSZ – Hardangerfjord Shear Zone; KSZ – Karmøy Shear Zone; SSZ – Stavanger Shear Zone.

Figure 5 – TWT structure maps of shallower structural levels, see Figures 2 and 3 for equivalent stratigraphic horizons. A) TWT structure map of the Middle Jurassic (Base RP2) surface. The main structural lows are the South, Central, North Viking Graben and the Sogn Graben, deepening to the north. B) TWT structure map of the Base Cretaceous Unconformity (Near Top-RP2) horizon, showing the main structural lows in the Viking Graben. Note the additional low centred above the Stord Basin.

C) TWT structure map of the Top Cretaceous (Post-rift) surface. This surface shows little faulting aside from the Western Boundary Fault along its western margin and is dominated by a N-trending depression, which widens northwards.

Figure 6 – Time-thickness map for Rift Phase 1, calculated between the Base RP1 and Base RP2 surfaces. Calculated depocentres are shown on the left and interpretation on the right. Red lines show the location of the offshore extensions of major Devonian structures (after Fazlikhani et al. (2017)). NSZ – Ninian Shear Zone; BSZ – Brent Shear Zone; TSZ – Tampen Shear Zone; LSZ – Lomre Shear Zone; USZ – Utsira Shear Zone; ØSZ – Øygarden Shear Zone; HSZ – Hardangerfjord Shear Zone; KSZ – Karmøy Shear Zone; WBF – Western Boundary Fault; TF – Tusse Fault; VF – Vette Fault; ØF (C and S) – Øygarden Fault (Central and Southern); ÅF - Åsta Fault

Figure 7 – Uninterpreted and interpreted seismic section across the Stord Basin, see Figure 4 for location. The section shows major RP1 activity along basin-bounding faults, which appear to root down onto the underlying Utsira and Øygarden/Hardangerfjord Shear zones at depth. Westwards progradation of the Hardangerfjord Delta can be observed in the Jurassic. Data courtesy of TGS (NSR06-31158.0016678).

Figure 8 – Uninterpreted and interpreted seismic section across the Northern Horda Platform, see Figure 4 for location. The W-dipping Tusse, Vette and Øygarden Faults show activity in the Triassic (RP1) and Cretaceous (Late-syn- to Post-RP2) with no activity in the Late Jurassic (RP2). The Øygarden and Vette Faults also show evidence of reflectivity below the Base RP1 surface. Data courtesy of TGS (NSR06-31182.0009614).

Figure 9 – Uninterpreted and interpreted section from across the East Shetland Basin, see Figure 4 for location. E-dipping faults appear to merge beneath the East Shetland Basin and may link to the Tampen and Ninian shear zones in this area. The depth to the Base RP1 surface becomes uncertain to the east, beneath the North Viking Graben. Data courtesy of TGS (NSR06-21188.0010680)

Figure 10 – Time-thickness and activity maps for RP2, calculated between the Base RP2 and BCU (Near Top-RP2) surfaces. Dashed diagonal lines correspond to areas of non-deposition or erosion. Green lines represent the offshore location of Devonian shear zones, with structures referred to in the text labelled. The Upper Jurassic Hardangerfjord and Sognefjord deltaic sequences are shown in brown. TSZ – Tampen Shear Zone; LSZ – Lomre Shear Zone; WBF – Western Boundary Fault; VF – Vette Fault.

Figure 11 – Time-thickness map for Late-syn- to Post-RP2, calculated between the BCU (Near Top-RP2) and top Lower Cretaceous (Post-rift) surfaces. Devonian shear zones are highlighted by light blue lines. The thickness of strata increases northwards into the Sogn Graben and Marulk and Magnus Basins. Note the reactivation of the faults across the Northern Horda Platform. TSZ – Tampen Shear Zone; LSZ – Lomre Shear Zone; WBF – Western Boundary Fault; TF – Tusse Fault; VF – Vette Fault; ØF (C) – Øygarden Fault (Central).

Figure 12 – Uninterpreted and interpreted seismic sections across the Sogn Graben, see Figure 4 for location. The Sogn Graben displays some activity during RP1 but is mainly active in RP2. The eastern margin of the graben is active during RP2 and Late-syn- to Post-RP2 intervals. No RP1 strata are present across the Måløy Slope, which shows RP2 activity. Data courtesy of CGG (Horda Platform Broadband 3D seismic volume)

Figure 13 – Regional model for the multiphase evolution of the northern North Sea rift. A) Major RP1 depocentres in the Stord Basin and East Shetland Basin are delineated by and somewhat controlled by the Devonian shear zones. B) RP2 activity localises onto the Viking and Sogn Grabens and the East Shetland Basin, with negligible activity observed across the Stord Basin and Northern Horda Platform, east of the Utsira High and the Lomre Shear Zone. C) Rift activity migrates northwards during the later stages and following RP2. Activity occurs along the NE-trending Marulk and Magnus Basins in

the north of the area with local flexure related reactivation of faults across the Northern Horda Platform.

Figure 14 – Schematic model showing the difference in activity between the northern and southern sections of the study area, and the role of the Utsira High. A) During RP1, rift activity in the north is distributed over a wide area, forming a wide rift and resulting in uniform lithospheric thinning. In the south, extension is localised into two segments either side of the relatively unfaulted Utsira High, producing relatively thin lithosphere beneath the rift segments and leaving relatively thicker lithosphere beneath the Utsira High. B) During RP2, the uniformly thinned lithosphere in the north focusses activity towards the axis, creating a localised rift centred across the Viking Graben. In the south, the modified lithospheric structure remnant from RP1 focusses activity along one rift segment, the South Viking Graben, buttressed by the thicker lithosphere of the Utsira High; whilst the rift segment on the opposite side to the Utsira High, the Stord Basin, becomes abandoned.

Figure 15 – 3D box model highlighting the range of possible interactions between pre-existing basement structures and rift related faults throughout multiple rift phases. Shear zones may locally perturb the regional stress field, causing incipient faults to locally align along these structures. Faults may also exploit internal anisotropies within shear zones, or where the shear zones are oriented at a relatively high angle, be segmented by them. In some instances, shear zones may form the limit to activity during later rift events. Granite-cored bodies are often located in the footwalls of faults and are typically resistant to extension.

Figure S1 – Uninterpreted seismic sections of Figure 3.

Table A1 – Summary of seismic surveys and their acquisition parameters as used in this study. From Fazlikhani et al. (2017).

Table A2 – Table showing basement penetrating exploration wells used in this study, after Fazlikhani et al. (2017). Depths shown are measured depth (MD) from the Kelly Bushing (KB) datum. Well information shown by asterisk is from Bassett (2003) and Marshall & Hewett (2003).

Acknowledgements

This contribution forms part of the MultiRift Project funded by the Research Council of Norway (PETROMAKS project215591/E30) and Equinor to the University of Bergen and partners Imperial College, University of Manchester and University of Oslo. Thanks to TGS and CGG for permission to publish the seismic data and to Schlumberger for providing academic licenses for the use of Petrel at the University of Bergen and the University of Durham. We would also like to thank the VISTA program for supporting the professorship of Gawthorpe and a visiting researcher scholarship to Phillips at the University of Bergen, and also the Leverhulme Trust for supporting Phillips through a Leverhulme Early Career Fellowship at the University of Durham.

References

Andersen, T.B. & Jamtveit, B. 1990. Uplift of deep crust during orogenic extensional collapse: A model based on field studies in the Sogn-Sunnfjord Region of western Norway. *Tectonics*, **9**, 1097-1111.

Bartholomew, I.D., Peters, J.M. & Powell, C.M. 1993. Regional structural evolution of the North Sea: oblique slip and the reactivation of basement lineaments. *Geological Society, London, Petroleum Geology Conference series*, **4**, 1109-1122, http://doi.org/10.1144/0041109.

Bassett, M. 2003. Sub-Devonian geology. *The Millennium Atlas: Petroleum Geology of the Central and Northern North Sea. Geological Society, London*, **61**, 63.

Bell, R.E., Jackson, C.A.L., Whipp, P.S. & Clements, B. 2014. Strain migration during multiphase extension: Observations from the northern North Sea. *Tectonics*, **33**, 1936-1963, http://doi.org/10.1002/2014TC003551.

Bird, P.C., Cartwright, J.A. & Davies, T.L. 2014. Basement reactivation in the development of rift basins: an example of reactivated Caledonide structures in the West Orkney Basin. *Journal of the Geological Society*, **172**, 77-85, http://doi.org/10.1144/jgs2013-098.

BIRPS & ECORS. 1986. Deep seismic reflection profiling between England, France and Ireland. *Journal of the Geological Society, London*, **143**, 45-52.

Bladon, A.J., Clarke, S.M. & Burley, S.D. 2015. Complex rift geometries resulting from inheritance of pre-existing structures: Insights and regional implications from the Barmer Basin rift. *Journal of Structural Geology*, **71**, 136-154, http://doi.org/https://doi.org/10.1016/j.jsg.2014.09.017.

Bøe, R., Fossen, H. & Smelror, M. 2010. Mesozoic sediments and structures onshore Norway and in the coastal zone. *Norges geologiske undersøkelse Bulletin*, **450**, 15-32.

Boone, S.C., Seiler, C., Kohn, B.P., Gleadow, A.J.W., Foster, D.A. & Chung, L. 2018. Influence of Rift Superposition on Lithospheric Response to East African Rift System Extension: Lapur Range, Turkana, Kenya. *Tectonics*, **37**, 182-207, http://doi.org/10.1002/2017TC004575.

Bott, M.H.P., Day, A.A. & Massonsmith, D. 1958. The Geological Interpretation of Gravity and Magnetic Surveys in Devon and Cornwall. *Philosophical Transactions of the Royal Society of London Series a-Mathematical and Physical Sciences*, **251**, 161-191, http://doi.org/10.1098/rsta.1958.0013.

Brekke, H. & Riis, F. 1987. Tectonics and basin evolution of the Norwegian shelf between 62 N and 72 N. *Norsk Geologisk Tidsskrift*, **67**, 295-322.

Brun, J.P. & Tron, V. 1993. Development of the North Viking Graben - Inferences from Laboratory Modeling. *Sedimentary Geology*, **86**, 31-51, http://doi.org/10.1016/0037-0738(93)90132-O.

Brune, S., Corti, G. & Ranalli, G. 2017. Controls of inherited lithospheric heterogeneity on rift linkage: Numerical and analog models of interaction between the Kenyan and Ethiopian rifts across the Turkana depression. *Tectonics*, **36**, 1767-1786, http://doi.org/10.1002/2017TC004739.

Chadwick, R.A., Pharaoh, T.C. & Smith, N.J.P. 1989. Lower crustal heterogeneity beneath Britain from deep seismic reflection data. *Journal of the Geological Society*, **146**, 617, http://doi.org/10.1144/gsjgs.146.4.0617.

Chattopadhyay, A. & Chakra, M. 2013. Influence of pre-existing pervasive fabrics on fault patterns during orthogonal and oblique rifting: An experimental approach. *Marine and Petroleum Geology*, **39**, 74-91, http://doi.org/http://dx.doi.org/10.1016/j.marpetgeo.2012.09.009.

Christiansson, P., Faleide, J.I. & Berge, A.M. 2000. Crustal structure in the northern North Sea: an integrated geophysical study. *Geological Society, London, Special Publications*, **167**, 15, http://doi.org/10.1144/GSL.SP.2000.167.01.02.

Claringbould, J.S., Bell, R.E., Jackson, C.A.L., Gawthorpe, R.L. & Odinsen, T. 2017. Pre-existing normal faults have limited control on the rift geometry of the northern North Sea. *Earth and Planetary Science Letters*, http://doi.org/https://doi.org/10.1016/j.epsl.2017.07.014.

Collanega, L., Jackson, C.A.L., Bell, R.E., Coleman, A.J., Lenhart, A. & Breda, A. 2018. Normal fault growth influenced by basement fabrics: the importance of preferential nucleation from pre-existing structures. *Basin Research*, **0**, http://doi.org/10.1111/bre.12327.

Corti, G. 2008. Control of rift obliquity on the evolution and segmentation of the main Ethiopian rift. *Nature Geoscience*, **1**, 258, http://doi.org/10.1038/ngeo160

https://www.nature.com/articles/ngeo160#supplementary-information.

Corti, G. 2009. Continental rift evolution: From rift initiation to incipient break-up in the Main Ethiopian Rift, East Africa. *Earth-Science Reviews*, **96**, 1-53, http://doi.org/https://doi.org/10.1016/j.earscirev.2009.06.005.

Corti, G., van Wijk, J., Cloetingh, S. & Morley, C.K. 2007. Tectonic inheritance and continental rift architecture: Numerical and analogue models of the East African Rift system. *Tectonics*, **26**, http://doi.org/10.1029/2006tc002086.

Coward, M.P. 1990. The Precambrian, Caledonian and Variscan framework to NW Europe. *Geological Society, London, Special Publications*, **55**, 1-34, http://doi.org/10.1144/gsl.sp.1990.055.01.01.

Coward, M.P. 1995. Structural and tectonic setting of the Permo-Triassic basins of northwest Europe. *Geological Society, London, Special Publications*, **91**, 7-39, http://doi.org/10.1144/gsl.sp.1995.091.01.02.

Coward, M.P., Dewey, J.F., Hempton, M. & Holroyd, J. 2003. Tectonic evolution. *In*: Evans, D., Graham, C., Armour, A. & Bathurst, P. (eds.) *The Millenium Atlas: petroleum geology of the central and northern North Sea*, Geological Society of London.

Cowie, P.A., Underhill, J.R., Behn, M.D., Lin, J. & Gill, C.E. 2005. Spatio-temporal evolution of strain accumulation derived from multi-scale observations of Late Jurassic rifting in the northern North Sea: A critical test of models for lithospheric extension. *Earth and Planetary Science Letters*, **234**, 401-419, http://doi.org/10.1016/j.epsl.2005.01.039.

Critchley, M.F. 1984. Variscan tectonics of the Alston block, northern England. *Geological Society, London, Special Publications*, **14**, 139, http://doi.org/10.1144/GSL.SP.1984.014.01.14.

Daly, M.C., Chorowicz, J. & Fairhead, J.D. 1989. Rift basin evolution in Africa: the influence of reactivated steep basement shear zones. *Geological Society, London, Special Publications*, **44**, 309, http://doi.org/10.1144/GSL.SP.1989.044.01.17.

Davies, R.J., Turner, J.D. & Underhill, J.R. 2001. Sequential dip-slip fault movement during rifting: a new model for the evolution of the Jurassic trilete North Sea rift system. *Petroleum Geoscience*, **7**, 371, http://doi.org/10.1144/petgeo.7.4.371.

Davies, R.J., O'Donnell, D., Bentham, P.N., Gibson, J.P.C., Curry, M.R., Dunay, R.E. & Maynard, J.R. 1999. The origin and genesis of major Jurassic unconformities within the triple junction area of the North Sea, UK. *Geological Society, London, Petroleum Geology Conference series*, **5**, 117.

de Castro, D.L., de Oliveira, D.C. & Gomes Castelo Branco, R.M. 2007. On the tectonics of the Neocomian Rio do Peixe Rift Basin, NE Brazil: Lessons from gravity, magnetics, and radiometric data. *Journal of South American Earth Sciences*, **24**, 184-202, http://doi.org/https://doi.org/10.1016/j.jsames.2007.04.001.

Deng, C., Gawthorpe, R.L., Finch, E. & Fossen, H. 2017a. Influence of a pre-existing basement weakness on normal fault growth during oblique extension: Insights from discrete element modeling. *Journal of Structural Geology*, http://doi.org/https://doi.org/10.1016/j.jsg.2017.11.005.

Deng, C., Fossen, H., Gawthorpe, R.L., Rotevatn, A., Jackson, C.A.L. & FazliKhani, H. 2017b. Influence of fault reactivation during multiphase rifting: The Oseberg area, northern North Sea rift. *Marine and Petroleum Geology*, **86**, 1252-1272, http://doi.org/http://dx.doi.org/10.1016/j.marpetgeo.2017.07.025.

Donato, J. & Tully, M. 1982. A proposed granite batholith along the western flank of the North Sea Viking Graben. *Geophysical Journal International*, **69**, 187-195.

Donato, J.A., Martindale, W. & Tully, M.C. 1983. Buried granites within the Mid North Sea High. *Journal of the Geological Society*, **140**, 825, http://doi.org/10.1144/gsjgs.140.5.0825.

Dore, A.G., Lundin, E.R., Fichler, C. & Olesen, O. 1997. Patterns of basement structure and reactivation along the NE Atlantic margin. *Journal of the Geological Society*, **154**, 85-92, http://doi.org/DOI 10.1144/gsjgs.154.1.0085.

Dreyer, T., Whitaker, M., Dexter, J., Flesche, H. & Larsen, E. 2005. From spit system to tide-dominated delta: integrated reservoir model of the Upper Jurassic Sognefjord Formation on the Troll West Field. *Geological Society, London, Petroleum Geology Conference series*, **6**, 423, http://doi.org/10.1144/0060423.

Duffy, O.B., Bell, R.E., Jackson, C.A.L., Gawthorpe, R.L. & Whipp, P.S. 2015. Fault growth and interactions in a multiphase rift fault network: Horda Platform, Norwegian North Sea. *Journal of Structural Geology*, **80**, 99-119, http://doi.org/http://dx.doi.org/10.1016/j.jsg.2015.08.015.

Ebinger, C., Djomani, Y.P., Mbede, E., Foster, A. & Dawson, J.B. 1997. Rifting Archaean lithosphere: the Eyasi-Manyara-Natron rifts, East Africa. *Journal of the Geological Society*, **154**, 947, http://doi.org/10.1144/gsjgs.154.6.0947.

Evans, D. 2003. *The Millennium Atlas: Petroleum Geology of the Central and Northern North Sea;[a Project of the Geological Society of London, the Geological Survey of Denmark and Greenland and the Norwegian Petroleum Society]*.

Evans, D.J., Rowley, W.J., Chadwick, R.A., Kimbell, G.S. & Millward, D. 1994. Seismic reflection data and the internal structure of the Lake District batholith, Cumbria, northern England. *Proceedings of the Yorkshire Geological and Polytechnic Society*, **50**, 11, http://doi.org/10.1144/pygs.50.1.11.

Færseth, R.B. 1996. Interaction of Permo-Triassic and Jurassic extensional fault-blocks during the development of the northern North Sea. *Journal of the Geological Society*, **153**, 931-944, http://doi.org/10.1144/gsjgs.153.6.0931.

Færseth, R.B. & Ravnås, R. 1998. Evolution of the Oseberg fault-block in context of the northern north sea structural framework. *Marine and Petroleum Geology*, **15**, 467-490, http://doi.org/https://doi.org/10.1016/S0264-8172(97)00046-9.

Færseth, R.B., Gabrielsen, R.H. & Hurich, C.A. 1995. Influence of basement in structuring of the North Sea basin, offshore southwest Norway. *Norsk Geologisk Tidsskrift*, **75**, 105-119.

Færseth, R.B., Knudsen, B.E., Liljedahl, T., Midbøe, P.S. & Søderstrøm, B. 1997. Oblique rifting and sequential faulting in the Jurassic development of the northern North Sea. *Journal of Structural Geology*, **19**, 1285-1302, http://doi.org/http://dx.doi.org/10.1016/S0191-8141(97)00045-X.

Fazlikhani, H., Fossen, H., Gawthorpe, R., Faleide, J.I. & Bell, R.E. 2017. Basement structure and its influence on the structural configuration of the northern North Sea rift. *Tectonics*, **36**, 1151-1177, http://doi.org/10.1002/2017tc004514.

Fichler, C., Odinsen, T., Rueslåtten, H., Olesen, O., Vindstad, J.E. & Wienecke, S. 2011. Crustal inhomogeneities in the Northern North Sea from potential field modeling: Inherited structure and serpentinites? *Tectonophysics*, **510**, 172-185, http://doi.org/https://doi.org/10.1016/j.tecto.2011.06.026.

Fossen, H. 1992. The role of extensional tectonics in the Caledonides of south Norway. *Journal of Structural Geology*, **14**, 1033-1046.

Fossen, H. 2010. Extensional tectonics in the North Atlantic Caledonides: a regional view. *Geological Society, London, Special Publications*, **335**, 767-793, http://doi.org/10.1144/sp335.31.

Fossen, H. & Rykkelid, E. 1992. Postcollisional extension of the Caledonide orogen in Scandinavia: Structural expressions and tectonic significance. *Geology*, **20**, 737, http://doi.org/10.1130/0091-7613(1992)020<0737:peotco>2.3.co;2.

Fossen, H. & Dunlap, J.W. 1998. Timing and kinematics of Caledonian thrusting and extensional collapse, southern Norway: evidence from 40Ar/39Ar thermochronology. *Journal of Structural Geology*, **20**, 765-781.

Fossen, H. & Dunlap, W.J. 1999. On the age and tectonic significance of Permo-Triassic dikes in the Bergen-Sunnhordland region, southwestern Norway. *Norsk Geologisk Tidsskrift*, **79**, 169-178.

Fossen, H. & Hurich, C.A. 2005. The Hardangerfjord Shear Zone in SW Norway and the North Sea: a large-scale low-angle shear zone in the Caledonian crust. *Journal of the Geological Society*, **162**, 675-687, http://doi.org/10.1144/0016-764904-136.

Fossen, H., Gabrielsen, R.H., Faleide, J.I. & Hurich, C.A. 2014. Crustal stretching in the Scandinavian Caledonides as revealed by deep seismic data. *Geology*, **42**, 791-794, http://doi.org/10.1130/g35842.1.

Fossen, H., Khani, H.F., Faleide, J.I., Ksienzyk, A.K. & Dunlap, W.J. 2016. Post-Caledonian extension in the West Norway–northern North Sea region: the role of structural inheritance. *Geological Society, London, Special Publications*, **439**, http://doi.org/https://doi.org/10.1144/SP439.6.

Gabrielsen, R.H., Fossen, H., Faleide, J.I. & Hurich, C.A. 2015. Mega-scale Moho relief and the structure of the lithosphere on the eastern flank of the Viking Graben, offshore southwestern Norway. *Tectonics*, **34**, 803-819.

Gabrielsen, R.H., Kyrkjebø, R., Faleide, J.I., Fjeldskaar, W. & Kjennerud, T. 2001. The Cretaceous post-rift basin configuration of the northern North Sea. *Petroleum Geoscience*, **7**, 137-154.

Gee, D.G., Fossen, H., Henriksen, N. & Higgins, A.K. 2008. From the early Paleozoic platforms of Baltica and Laurentia to the Caledonide Orogen of Scandinavia and Greenland. *Episodes*, **31**, 44-51.

Gontijo-Pascutti, A., Bezerra, F.H.R., Terra, E.L. & Almeida, J.C.H. 2010. Brittle reactivation of mylonitic fabric and the origin of the Cenozoic Rio Santana Graben, southeastern Brazil. *Journal of South American Earth Sciences*, **29**, 522-536, http://doi.org/http://dx.doi.org/10.1016/j.jsames.2009.06.007.

Heeremans, M. & Faleide, J.I. 2004. Late Carboniferous-Permian tectonics and magmatic activity in the Skagerrak, Kattegat and the North Sea. *Geological Society, London, Special Publications*, **223**, 157-176.

Heeremans, M., Faleide, J.I. & Larsen, B.T. 2004. Late Carboniferous -Permian of NW Europe: an introduction to a new regional map. *Geol Soc London, Special Publication*, **223**, 75-88.

Heilman, E., Kolawole, F., Atekwana, E.A. & Mayle, M. 2019. Controls of Basement Fabric on the Linkage of Rift Segments. *Tectonics*, **0**, http://doi.org/10.1029/2018TC005362.

Henstra, G.A., Rotevatn, A., Gawthorpe, R.L. & Ravnås, R. 2015. Evolution of a major segmented normal fault during multiphase rifting: The origin of plan-view zigzag geometry. *Journal of Structural Geology*, **74**, 45-63, http://doi.org/https://doi.org/10.1016/j.jsg.2015.02.005.

Henstra, G.A., Berg Kristensen, T., Rotevatn, A. & Gawthorpe, R.L. 2019. How do pre-existing normal faults influence rift geometry? A comparison of adjacent basins with contrasting underlying structure on the Lofoten Margin, Norway. *Basin Research*, **0**, http://doi.org/10.1111/bre.12358.

Hossack, J.R. & Cooper, M.A. 1986. Collision tectonics in the Scandinavian Caledonides. *Geological Society, London, Special Publications*, **19**, 285-304, http://doi.org/10.1144/gsl.Sp.1986.019.01.16.

Howell, L., Egan, S., Leslie, G. & Clarke, S. 2019. Structural and geodynamic modelling of the influence of granite bodies during lithospheric extension: Application to the Carboniferous basins of northern England. *Tectonophysics*, http://doi.org/https://doi.org/10.1016/j.tecto.2019.02.008.

Hurich, C. & Kristoffersen, Y. 1988. Deep structure of the Caledonide orogen in southern Norway: new evidence from marine seismic reflection profiling. *Norges Geologiske Undersøkelse Special Publication*, **3**, 96-101.

Jackson, C.A.L. & Lewis, M.M. 2013. Physiography of the NE margin of the Permian Salt Basin: new insights from 3D seismic reflection data. *Journal of the Geological Society*, **170**, 857-860, http://doi.org/10.1144/jgs2013-026.

Jackson, C.A.L. & Lewis, M.M. 2016. Structural style and evolution of a salt-influenced rift basin margin; the impact of variations in salt composition and the role of polyphase extension. *Basin Research*, **28**, 81-102, http://doi.org/10.1111/bre.12099.

Jackson, C.A.L. & Stewart, S.A. 2017. Chapter 8 - Composition, Tectonics, and Hydrocarbon Significance of Zechstein Supergroup Salt on the United Kingdom and Norwegian Continental Shelves: A Review. *In*: Soto, J.I., Flinch, J.F. & Tari, G. (eds) *Permo-Triassic Salt Provinces of Europe, North Africa and the Atlantic Margins*. Elsevier, 175-201.

Kimbell, G.S., Young, B., Millward, D. & Crowley, Q.G. 2010. The North Pennine batholith (Weardale Granite) of northern England: new data on its age and form. *Proceedings of the Yorkshire Geological Society*, **58**, 107, http://doi.org/10.1144/pygs.58.1.273.

Kirkpatrick, J.D., Bezerra, F.H.R., Shipton, Z.K., Do Nascimento, A.F., Pytharouli, S.I., Lunn, R.J. & Soden, A.M. 2013. Scale-dependent influence of pre-existing basement shear zones on rift faulting: a case study from NE Brazil. *Journal of the Geological Society*, **170**, 237, http://doi.org/10.1144/jgs2012-043.

Klemperer, S. & Hobbs, R. 1991. *The BIRPS Atlas: Deep seismic reflection profiles around the British Isles*. Cambridge University Press.

Koopmann, H., Brune, S., Franke, D. & Breuer, S. 2014. Linking rift propagation barriers to excess magmatism at volcanic rifted margins. *Geology*, **42**, 1071-1074, http://doi.org/10.1130/G36085.1.

Kristoffersen, Y. 1978. Sea-floor spreading and the early opening of the North Atlantic. *Earth and Planetary Science Letters*, **38**, 273-290, http://doi.org/https://doi.org/10.1016/0012-821X(78)90101-2.

Kyrkjebø, R., Gabrielsen, R. & Faleide, J. 2004. Unconformities related to the Jurassic–Cretaceous synrift–post-rift transition of the northern North Sea. *Journal of the Geological Society*, **161**, 1-17.

Lenhart, A., Jackson, C.A.L., Bell, R.E., Duffy, O.B., Gawthorpe, R.L. & Fossen, H. 2019. Structural architecture and composition of crystalline basement offshore west Norway. http://doi.org/10.1130/L668.1.

Lundmark, A.M., Saether, T. & Sorlie, R. 2013. Ordovician to Silurian magmatism on the Utsira High, North Sea: implications for correlations between the onshore and offshore Caledonides. *Geological Society, London, Special Publications*, **390**, 513-523, http://doi.org/10.1144/sp390.21.

Marshall, J. & Hewett, A. 2003. Devonian. Geological Society of London.

McClay, Norton, M.G., Coney, P. & Davis, G.H. 1986. Collapse of the Caledonian orogen and the Old Red Sandstone. *Nature*, **323**, 147-149.

McKerrow, W.S., MacNiocaill, C. & Dewey, J.F. 2000. The Caledonian Orogeny redefined. *Journal of the Geological Society, London*, **157**, 1149-1154.

Milnes, A.G., Wennberg, O.P., Skår, Ø. & Koestler, A.G. 1997. Contraction, extension and timing in the South Norwegian Caledonides: the Sognefjord transect. *Geological Society, London, Special Publications*, **121**, 123, http://doi.org/10.1144/GSL.SP.1997.121.01.06.

Morley, C.K. 2010. Stress re-orientation along zones of weak fabrics in rifts: An explanation for pure extension in 'oblique' rift segments? *Earth and Planetary Science Letters*, **297**, 667-673, http://doi.org/https://doi.org/10.1016/j.epsl.2010.07.022.

Morley, C.K. 2017. The impact of multiple extension events, stress rotation and inherited fabrics on normal fault geometries and evolution in the Cenozoic rift basins of Thailand. *Geological Society, London, Special Publications*, **439**, 413, http://doi.org/10.1144/SP439.3.

Morley, C.K., Haranya, C., Phoosongsee, W., Pongwapee, S., Kornsawan, A. & Wonganan, N. 2004. Activation of rift oblique and rift parallel pre-existing fabrics during extension and their effect on deformation style: examples from the rifts of Thailand. *Journal of Structural Geology*, **26**, 1803-1829, http://doi.org/https://doi.org/10.1016/j.jsg.2004.02.014.

Mortimer, E.J., Paton, D.A., Scholz, C.A. & Strecker, M.R. 2016. Implications of structural inheritance in oblique rift zones for basin compartmentalization: Nkhata Basin, Malawi Rift (EARS). *Marine and Petroleum Geology*, **72**, 110-121, http://doi.org/https://doi.org/10.1016/j.marpetgeo.2015.12.018.

Naliboff, J. & Buiter, S.J. 2015. Rift reactivation and migration during multiphase extension. *Earth and Planetary Science Letters*, **421**, 58-67.

Neumann, E.-R., Wilson, M., Heeremans, M., Spencer, E.A., Obst, K., Timmerman, M.J. & Kirstein, L. 2004. Carboniferous-Permian rifting and magmatism in southern Scandinavia, the North Sea and northern Germany: a review. *Geological Society, London, Special Publications*, **223**, 11-40, http://doi.org/10.1144/gsl.sp.2004.223.01.02.

Nixon, C.W., Sanderson, D.J., Dee, S.J., Bull, J.M., Humphreys, R.J. & Swanson, M.H. 2014. Fault interactions and reactivation within a normal-fault network at Milne Point, Alaska. *AAPG Bulletin*, **98**, 2081-2107.

NPD. 2014. Lithostratigraphic chart - Norwegian North Sea. *Norwegian Petroleum Directorate*

Odinsen, T., Reemst, P., Beek, P.V.D., Faleide, J.I. & Gabrielsen, R.H. 2000. Permo-Triassic and Jurassic extension in the northern North Sea: results from tectonostratigraphic forward modelling. *Geological Society, London, Special Publications*, **167**, 83-103, http://doi.org/10.1144/gsl.sp.2000.167.01.05.

Olsen, H., Briedis, N.A. & Renshaw, D. 2017. Sedimentological analysis and reservoir characterization of a multi-darcy, billion barrel oil field – The Upper Jurassic shallow marine sandstones of the Johan Sverdrup field, North Sea, Norway. *Marine and Petroleum Geology*, **84**, 102-134, http://doi.org/https://doi.org/10.1016/j.marpetgeo.2017.03.029.

Pascal, C., van Wijk, J.W., Cloetingh, S.A.P.L. & Davies, G.R. 2002. Effect of lithosphere thickness heterogeneities in controlling rift localization: Numerical modeling of the Oslo Graben. *Geophysical Research Letters*, **29**, 69-61-69-64, http://doi.org/doi:10.1029/2001GL014354.

Paton, D.A. & Underhill, J.R. 2004. Role of crustal anisotropy in modifying the structural and sedimentological evolution of extensional basins: the Gamtoos Basin, South Africa. *Basin Research*, **16**, 339-359, http://doi.org/10.1111/j.1365-2117.2004.00237.x.

Paton, D.A., Mortimer, E.J., Hodgson, N. & van der Spuy, D. 2016. The missing piece of the South Atlantic jigsaw: when continental break-up ignores crustal heterogeneity. *Geological Society, London, Special Publications*, **438**, SP438.438, http://doi.org/10.1144/SP438.8.

Patruno, S. & Reid, W. 2016. New plays on the Greater East Shetland Platform (UKCS Quadrants 3, 8-9, 14-16)–part 1: Regional setting and a working petroleum system. *first break*, **34**, 33-43.

Patruno, S., Reid, W., Berndt, C. & Feuilleaubois, L. 2019. Polyphase tectonic inversion and its role in controlling hydrocarbon prospectivity in the Greater East Shetland Platform and Mid North Sea High, UK. *Geological Society, London, Special Publications*, **471**, 177, http://doi.org/10.1144/SP471.9.

Peace, A., McCaffrey, K., Imber, J., van Hunen, J., Hobbs, R. & Wilson, R. 2017. The role of pre-existing structures during rifting, continental breakup and transform system development, offshore West Greenland. *Basin Research*, 373-394, http://doi.org/ https://doi.org/10.1111/bre.12257.

Pegrum, R.M. 1984. The extension of the Tornquist Zone in the Norwegian North Sea. *Norsk Geologisk Tidsskrift*, **64**, 39-68.

Philippon, M., Willingshofer, E., Sokoutis, D., Corti, G., Sani, F., Bonini, M. & Cloetingh, S. 2015. Slip re-orientation in oblique rifts. *Geology*, **43**, 147-150, http://doi.org/10.1130/G36208.1.

Phillips, T.B., Magee, C., Jackson, C.A.L. & Bell, R.E. 2017. Determining the three-dimensional geometry of a dike swarm and its impact on later rift geometry using seismic reflection data. *Geology*, **46**, 119-122, http://doi.org/10.1130/G39672.1.

Phillips, T.B., Jackson, C.A., Bell, R.E., Duffy, O.B. & Fossen, H. 2016. Reactivation of intrabasement structures during rifting: A case study from offshore southern Norway. *Journal of Structural Geology*, **91**, 54-73, http://doi.org/10.1016/j.jsg.2016.08.008.

Prosser, S. 1993. Rift-related linked depositional systems and their seismic expression. *Geological Society, London, Special Publications*, **71**, 35, http://doi.org/10.1144/GSL.SP.1993.071.01.03.

Quirie, A.K., Schofield, N., Hartley, A., Hole, M.J., Archer, S.G., Underhill, J.R., Watson, D. & Holford, S.P. 2018. The Rattray Volcanics: Middle Jurassic fissure volcanism in the UK Central North Sea. *Journal of the Geological Society*, jgs2018-2151, http://doi.org/10.1144/jgs2018-151.

Ragon, T., Nutz, A., Schuster, M., Ghienne, J.-F., Ruffet, G. & Rubino, J.-L. 2018. Evolution of the northern Turkana Depression (East African Rift System, Kenya) during the Cenozoic rifting: New insights from the Ekitale Basin (28-25.5 Ma). *Geological Journal*, **0**, http://doi.org/10.1002/gj.3339.

Rattey, R.P. & Hayward, A.B. 1993. Sequence stratigraphy of a failed rift system: the Middle Jurassic to Early Cretaceous basin evolution of the Central and Northern North Sea. *Geological Society, London, Petroleum Geology Conference 				series*, **4**, 215-249, http://doi.org/10.1144/0040215.

Ravnås, R. & Bondevik, K. 1997. Architecture and controls on Bathonian–Kimmeridgian shallow-marine synrift wedges of the Oseberg–Brage area, northern North Sea. *Basin Research*, **9**, 197-226, http://doi.org/10.1046/j.1365-2117.1997.00041.x.

Ravnås, R., Nøttvedt, A., Steel, R.J. & Windelstad, J. 2000. Syn-rift sedimentary architectures in the Northern North Sea. *Geological Society, London, Special Publications*, **167**, 133, http://doi.org/10.1144/GSL.SP.2000.167.01.07.

Reeve, M.T., Bell, R.E. & Jackson, C.A.L. 2013. Origin and significance of intra-basement seismic reflections offshore western Norway. *Journal of the Geological Society*, **171**, 1-4, http://doi.org/10.1144/jgs2013-020.

Reeve, M.T., Bell, R.E., Duffy, O.B., Jackson, C.A.L. & Sansom, E. 2015. The growth of non-colinear normal fault systems; What can we learn from 3D seismic reflection data? *Journal of Structural Geology*, **70**, 141-155, http://doi.org/http://dx.doi.org/10.1016/j.jsg.2014.11.007.

Rey, P., Burg, J.P. & Casey, M. 1997. The Scandinavian Caledonides and their relationship to the Variscan belt. *Geological Society, London, Special Publications*, **121**, 179, http://doi.org/10.1144/GSL.SP.1997.121.01.08.

Riber, L., Dypvik, H. & Sørlie, R. 2015. Altered basement rocks on the Utsira High and its surroundings, Norwegian North Sea. *Norwegian Journal of Geology*, **95**, 57-89.

Roberts, A., Yielding, G. & Badley, M. 1990. A kinematic model for the orthogonal opening of the late Jurassic North Sea rift system, Denmark-Mid Norway. *Tectonic Evolution of the North Sea Rifts. Clarendon Press, Oxford*, **180**, 199.

Roberts, A.M., Yielding, G., Kusznir, N.J., Walker, I.M. & Dorn-Lopez, D. 1995. Quantitative analysis of Triassic extension in the northern Viking Graben. *Journal of the Geological Society*, **152**, 15.

Roberts, D. 2003. The Scandinavian Caledonides: event chronology, palaeogeographic settings and likely modern analogues. *Tectonophysics*, **365**, 283-299, http://doi.org/10.1016/s0040-1951(03)00026-x.

Roberts, D.G., Thompson, M., Mitchener, B., Hossack, J., Carmichael, S. & BjØRnseth, H.M. 1999. Palaeozoic to Tertiary rift and basin dynamics: mid-Norway to the Bay of Biscay – a new context for hydrocarbon prospectivity in the deep water frontier. *Geological Society, London, Petroleum Geology Conference series*, **5**, 7, http://doi.org/10.1144/0050007.

Roffeis, C. & Corfu, F. 2013. Caledonian nappes of southern Norway and their correlation with Sveconorwegian basement domains. *Geological Society, London, Special Publications*, **390**, 193-221, http://doi.org/10.1144/sp390.13.

Rotevatn, A., Kristensen, T.B., Ksienzyk, A.K., Wemmer, K., Henstra, G.A., Midtkandal, I., Grundvåg, S.-A. & Andresen, A. 2018. Structural Inheritance and Rapid Rift-Length Establishment in a Multiphase Rift: The East Greenland Rift System and its Caledonian Orogenic Ancestry. *Tectonics*, **37**, 1858-1875, http://doi.org/doi:10.1029/2018TC005018.

Salomon, E., Koehn, D. & Passchier, C. 2015. Brittle reactivation of ductile shear zones in NW Namibia in relation to South Atlantic rifting. *Tectonics*, **34**, 70-85, http://doi.org/10.1002/2014tc003728.

Samsu, A., Cruden, A.R., Hall, M., Micklethwaite, S. & Denyszyn, S.W. 2019. The influence of basement faults on local extension directions: Insights from potential field geophysics and field observations. *Basin Research*, **0**, http://doi.org/10.1111/bre.12344.

Scisciani, V., Patruno, S., Tavarnelli, E., Calamita, F., Pace, P. & Iacopini, D. 2019. Multi-phase reactivations and inversions of Paleozoic-Mesozoic extensional basins during the Wilson Cycle: case studies from the North Sea (UK) and Northern Apennines (Italy). *Geological Society, London, Special Publications*, **470**, SP470-2017-2232, http://doi.org/10.1144/SP470-2017-232.

Seranne, M. & Seguret, M. 1987. The Devonian basins of western Norway: tectonics and kinematics of an extending crust. *Geological Society, London, Special Publications*, **28**, 537-548, http://doi.org/10.1144/gsl.Sp.1987.028.01.35.

Skyttä, P., Piippo, S., Kloppenburg, A. & Corti, G. 2019. 2. 45 Ga break-up of the Archaean continent in Northern Fennoscandia: Rifting dynamics and the role of inherited structures within the Archaean basement. *Precambrian Research*, http://doi.org/https://doi.org/10.1016/j.precamres.2019.02.004.

Slagstad, T., Davidsen, B. & Daly, J.S. 2011. Age and composition of crystalline basement rocks on the Norwegian continental margin: offshore extension and continuity of the Caledonian–Appalachian orogenic belt. *Journal of the Geological Society*, **168**, 1167, http://doi.org/10.1144/0016-76492010-136.

Slagstad, T., Roberts, N.M.W., Marker, M., Røhr, T.S. & Schiellerup, H. 2013. A non-collisional, accretionary Sveconorwegian orogen. *Terra Nova*, **25**, 30-37, http://doi.org/10.1111/ter.12001.

Smethurst, M.A. 2000. Land–offshore tectonic links in western Norway and the northern North Sea. *Journal of the Geological Society*, **157**, 769-781, http://doi.org/10.1144/jgs.157.4.769.

Sømme, T.O., Lunt, I. & Martinsen, O.J. 2013. Linking offshore stratigraphy to onshore paleotopography: The Late Jurassic–Paleocene evolution of the south Norwegian margin. *GSA Bulletin*, **125**, 1164-1186, http://doi.org/10.1130/B30747.1.

Sorento, T., Stemmerik, L. & Olaussen, S. 2018. Upper Permian carbonates at the northern edge of the Zechstein basin, Utsira High, Norwegian North Sea. *Marine and Petroleum Geology*, **89**, 635-652, http://doi.org/https://doi.org/10.1016/j.marpetgeo.2017.10.030.

Stewart, I.J., Rattey, R.P. & Vann, I.R. 1992. Structural style and the habitat of hydrocarbons in the North Sea. *In*: Larsen, R.M., Brekke, H., Larsen, B.T. & Talleraas, E. (eds) *Structural and Tectonic Modelling and its Application to Petroleum Geology*. Elsevier, Amsterdam, **1**, 197-220.

Stewart, S., Ries, A., Butler, R. & Graham, R. 2007. Salt tectonics in the North Sea Basin: a structural style template for seismic interpreters. *Special Publication-Geological Society of London*, **272**, 361.

Stewart, S.A. & Coward, M.P. 1995. Synthesis of salt tectonics in the southern North Sea, UK. *Marine and Petroleum Geology*, **12**, 457-475, http://doi.org/https://doi.org/10.1016/0264-8172(95)91502-G.

Ter Voorde, M., Færseth, R.B., Gabrielsen, R.H. & Cloetingh, S.A.P.L. 2000. Repeated lithosphere extension in the northern Viking Graben: a coupled or a decoupled rheology? *Geological Society, London, Special Publications*, **167**, 59.

Thon, A. 1980. Steep shear zones in the basement and associated deformation of the cover sequence on Karmøy, SW Norwegian Caledonides. *Journal of Structural Geology*, **2**, 75-80.

Tomasso, M., Underhill, J.R., Hodgkinson, R.A. & Young, M.J. 2008. Structural styles and depositional architecture in the Triassic of the Ninian and Alwyn North fields: Implications for basin development and prospectivity in the Northern North Sea. *Marine and Petroleum Geology*, **25**, 588-605, http://doi.org/https://doi.org/10.1016/j.marpetgeo.2007.11.007.

Tong, H. & Yin, A. 2011. Reactivation tendency analysis: A theory for predicting the temporal evolution of preexisting weakness under uniform stress state. *Tectonophysics*, **503**, 195-200, http://doi.org/https://doi.org/10.1016/j.tecto.2011.02.012.

Underhill, J.R. & Partington, M.A. 1993. Jurassic thermal doming and deflation in the North Sea: implications of the sequence stratigraphic evidence. 337-345, http://doi.org/10.1144/0040337.

Vasconcelos, D.L., Bezerra, F.H.R., Medeiros, W.E., de Castro, D.L., Clausen, O.R., Vital, H. & Oliveira, R.G. 2019. Basement fabric controls rift nucleation and postrift basin inversion in the continental margin of NE Brazil. *Tectonophysics*, **751**, 23-40, http://doi.org/https://doi.org/10.1016/j.tecto.2018.12.019.

Vetti, V.V. & Fossen, H. 2012. Origin of contrasting Devonian supradetachment basin types in the Scandinavian Caledonides. *Geology*, **40**, 571-574, http://doi.org/10.1130/g32512.1.

Wenker, S. & Beaumont, C. 2016. Effects of lateral strength contrasts and inherited heterogeneities on necking and rifting of continents. *Tectonophysics*, http://doi.org/https://doi.org/10.1016/j.tecto.2016.10.011.

Whipp, P.S., Jackson, C.A.L., Gawthorpe, R.L., Dreyer, T. & Quinn, D. 2014. Normal fault array evolution above a reactivated rift fabric; a subsurface example from the northern Horda Platform, Norwegian North Sea. *Basin Research*, **26**, 523-549, http://doi.org/10.1111/bre.12050.

Wiest, J.D., Jacobs, J., Ksienzyk, A.K. & Fossen, H. 2018. Sveconorwegian vs. Caledonian orogenesis in the eastern Øygarden Complex, SW Norway – Geochronology, structural constraints and tectonic implications. *Precambrian Research*, **305**, 1-18, http://doi.org/https://doi.org/10.1016/j.precamres.2017.11.020.

Wilson, M., Neumann, E.-R., Davies, G.R., Timmerman, M., Heeremans, M. & Larsen, B.T. 2004. Permo-Carboniferous magmatism and rifting in Europe: introduction. *Geological Society, London, Special Publications*, **223**, 1-10.

Youash, Y. 1969. Tension Tests on Layered Rocks. *Geological Society of America Bulletin*, **80**, 303-306, http://doi.org/Doi 10.1130/0016-7606(1969)80[303:Ttolr]2.0.Co;2.

Zang, A. & Stephansson, O. 2009. *Stress field of the Earth's crust*. Springer Science & Business Media.

Ziegler, P.A. 1992. North-Sea Rift System. *Tectonophysics*, **208**, 55-75, http://doi.org/10.1016/0040-1951(92)90336-5.

Figure 1

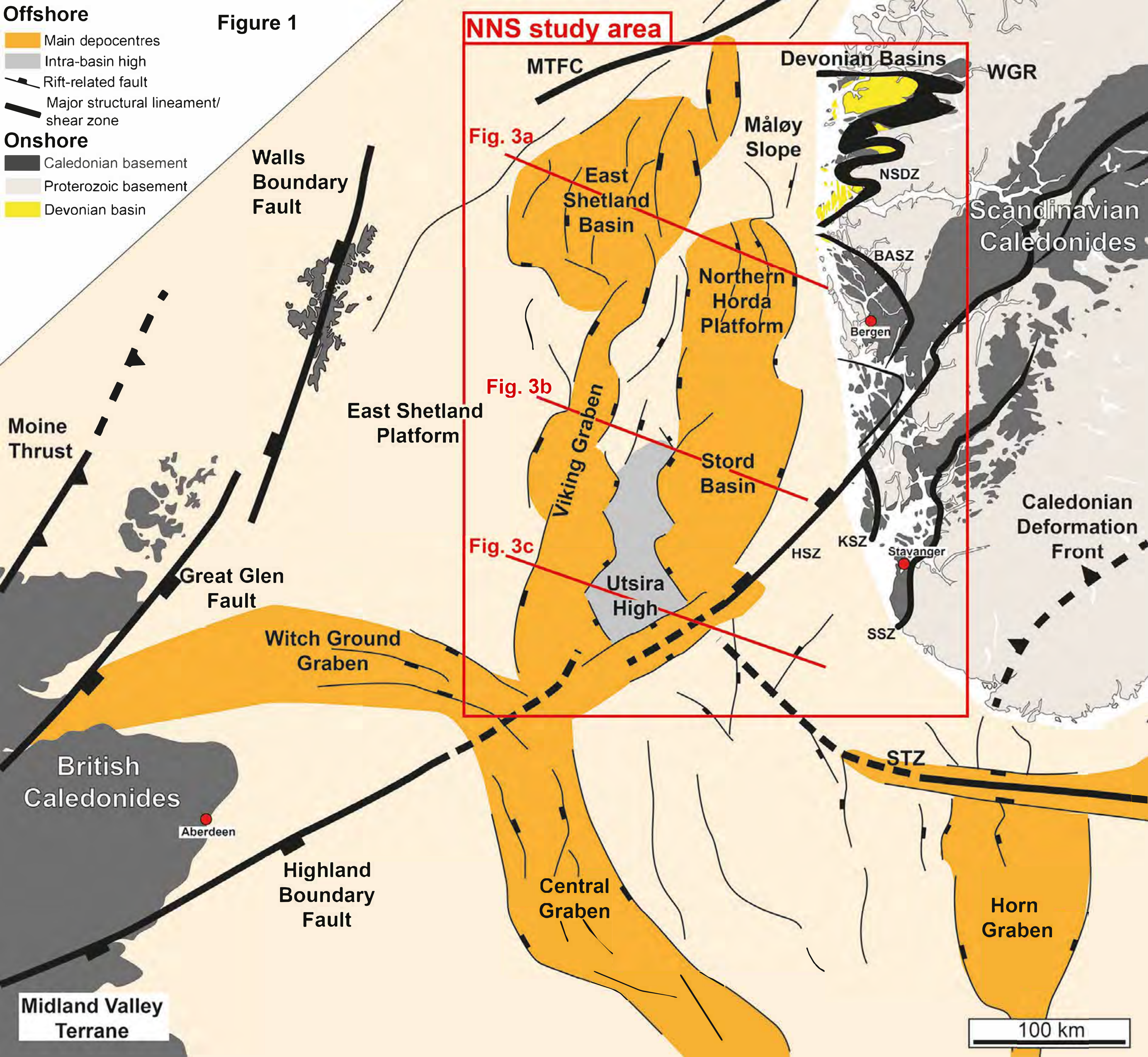
Offshore
Main depocentres
Intra-basin high
Rift-related fault
Major structural lineament/ shear zone
Onshore
Caledonian basement
Proterozoic basement
Devonian basin
NNS study area
MTFC
Devonian Basins
WGR
Fig. 3a
Måløy Slope
East Shetland Basin
NSDZ
Scandinavian Caledonides
Walls Boundary Fault
BASZ
Northern Horda Platform
Bergen
Fig. 3b
East Shetland Platform
Viking Graben
Moine Thrust
Stord Basin
Caledonian Deformation Front
Fig. 3c
HSZ
KSZ
Stavanger
Great Glen Fault
Utsira High
SSZ
Witch Ground Graben
STZ
British Caledonides
Aberdeen
Highland Boundary Fault
Central Graben
Horn Graben
Midland Valley Terrane
100 km

Figure 2

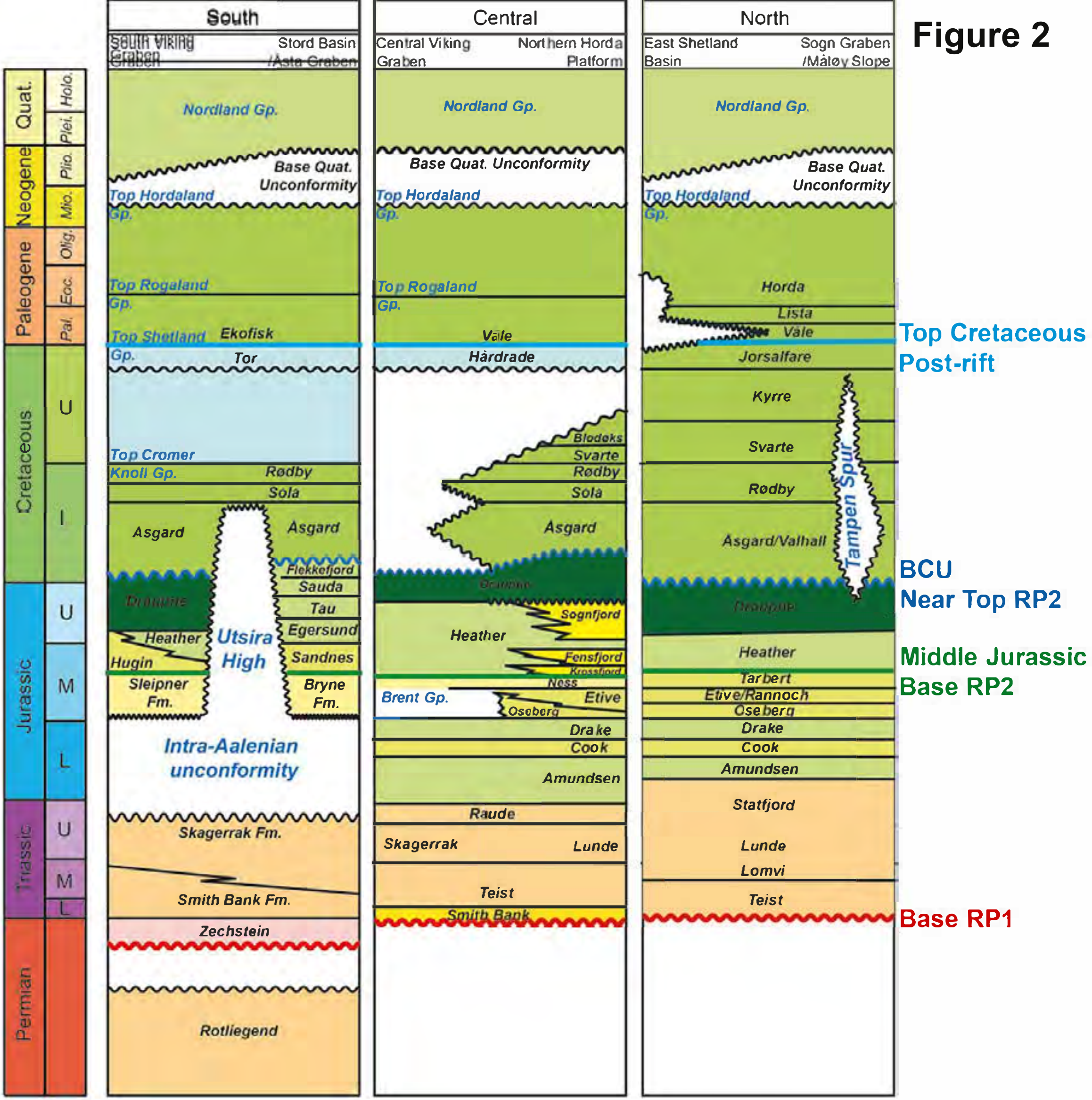

South
South Viking Graben
Stord Basin /Åsta Graben
Central
Central Viking Graben
Northern Horda Platform
North
East Shetland Basin
Sogn Graben /Måløy Slope
Quat.
Holo.
Plei.
Neogene
Plio.
Mio.
Paleogene
Olig.
Eoc.
Pal.
Cretaceous
U
l
Jurassic
U
M
L
Triassic
U
M
L
Permian
Nordland Gp.
Base Quat. Unconformity
Top Hordaland Gp.
Top Rogaland Gp.
Top Shetland Gp.
Ekofisk
Tor
Top Cromer Knoll Gp.
Rødby
Sola
Asgard
Flekkefjord
Sauda
Tau
Egersund
Sandnes
Draupne
Heather
Hugin
Sleipner Fm.
Bryne Fm.
Utsira High
Intra-Aalenian unconformity
Skagerrak Fm.
Smith Bank Fm.
Zechstein
Rotliegend
Våle
Hårdrade
Blodøks
Svarte
Sognfjord
Fensfjord
Krossfjord
Ness
Brent Gp.
Etive
Oseberg
Drake
Cook
Amundsen
Raude
Skagerrak
Lunde
Teist
Smith Bank
Horda
Lista
Jorsalfare
Kyrre
Asgard/Valhall
Tampen Spur
Tarbert
Etive/Rannoch
Statfjord
Lomvi
Top Cretaceous Post-rift
BCU Near Top RP2
Middle Jurassic Base RP2
Base RP1

Figure 3

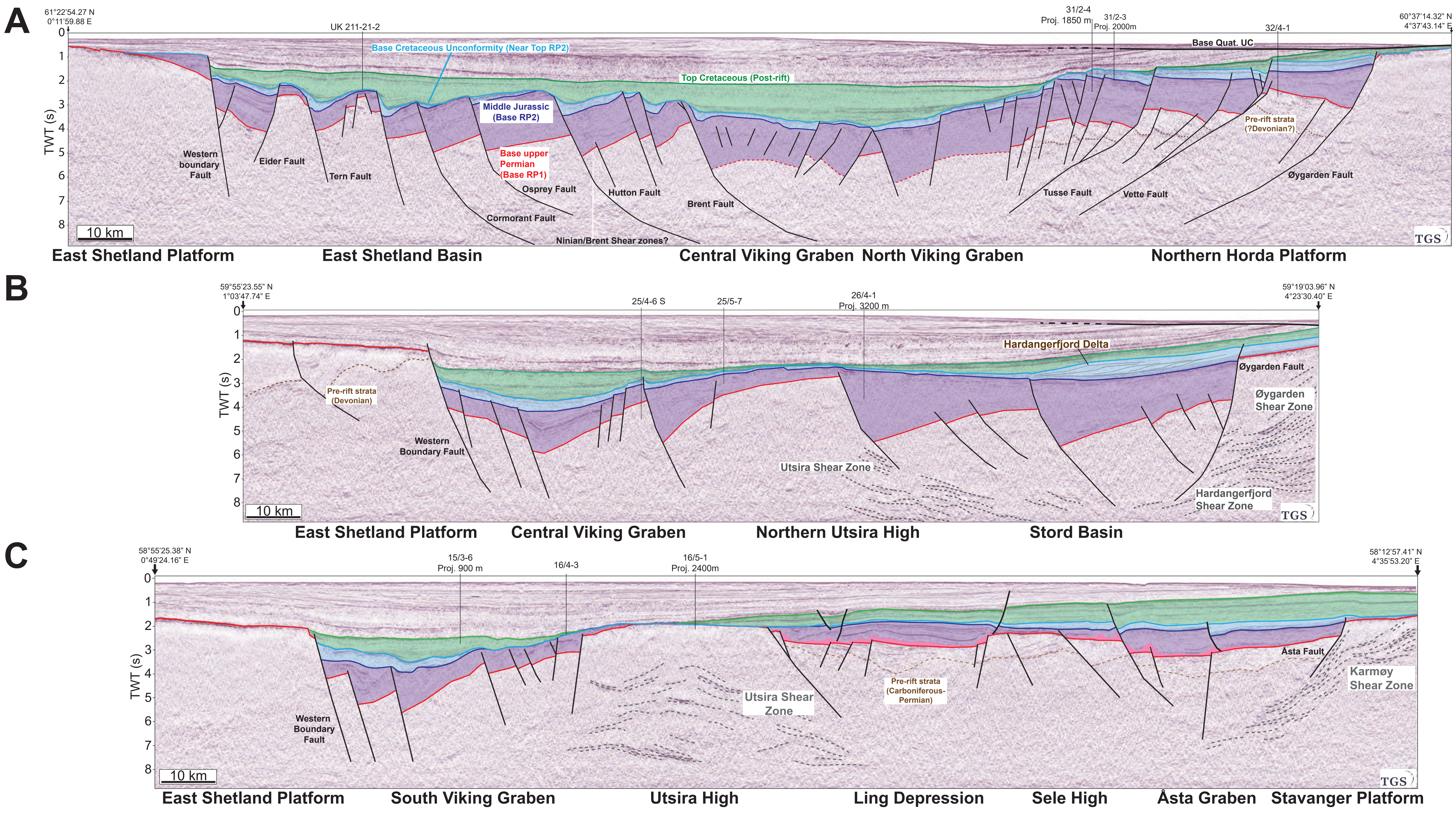
A
61°22'54.27" N
0°11'59.88" E
UK 211-21-2
31/2-4
Proj. 1850 m
31/2-3
Proj. 2000m
32/4-1
60°37'14.32" N
4°37'43.14" E
Base Quat. UC
Base Cretaceous Unconformity (Near Top RP2)
Top Cretaceous (Post-rift)
Middle Jurassic
(Base RP2)
Base upper
Permian
(Base RP1)
Pre-rift strata
(?Devonian?)
Western
boundary
Fault
Eider Fault
Tern Fault
Osprey Fault
Cormorant Fault
Hutton Fault
Ninian/Brent Shear zones?
Brent Fault
Tusse Fault
Vette Fault
Øygarden Fault
TWT (s)
10 km
TGS
East Shetland Platform
East Shetland Basin
Central Viking Graben
North Viking Graben
Northern Horda Platform
B
59°55'23.55" N
1°03'47.74" E
25/4-6 S
25/5-7
26/4-1
Proj. 3200 m
59°19'03.96" N
4°23'30.40" E
Hardangerfjord Delta
Øygarden Fault
Øygarden
Shear Zone
Pre-rift strata
(Devonian)
Western
Boundary Fault
Utsira Shear Zone
Hardangerfjord
Shear Zone
TWT (s)
10 km
TGS
East Shetland Platform
Central Viking Graben
Northern Utsira High
Stord Basin
C
58°55'25.38" N
0°49'24.16" E
15/3-6
Proj. 900 m
16/4-3
16/5-1
Proj. 2400m
58°12'57.41" N
4°35'53.20" E
Western
Boundary
Fault
Utsira Shear
Zone
Pre-rift strata
(Carboniferous-
Permian)
Åsta Fault
Karmøy
Shear Zone
TWT (s)
10 km
TGS
East Shetland Platform
South Viking Graben
Utsira High
Ling Depression
Sele High
Åsta Graben
Stavanger Platform

Figure 4

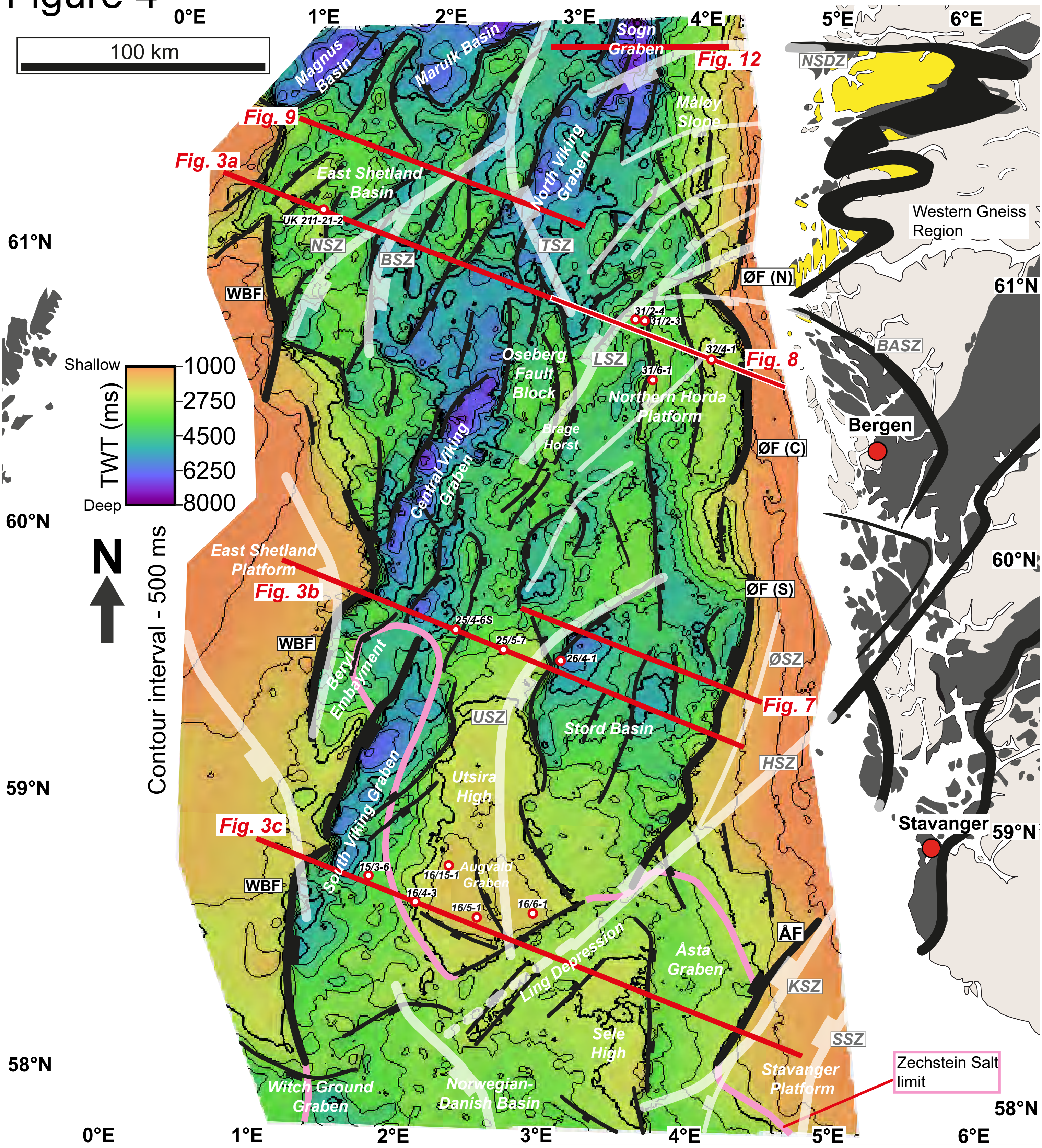

100 km
0°E
1°E
2°E
3°E
4°E
5°E
6°E
61°N
60°N
59°N
58°N
Shallow
Deep
TWT (ms)
1000
2750
4500
6250
8000
Contour interval - 500 ms
N
Magnus Basin
Marulk Basin
Sogn Graben
Fig. 12
Fig. 9
Fig. 3a
Fig. 8
Fig. 3b
Fig. 7
Fig. 3c
Måløy Slope
East Shetland Basin
North Viking Graben
UK 211-21-2
NSZ
BSZ
TSZ
WBF
ØF (N)
31/2-4
31/2-3
32/4-1
Oseberg Fault Block
LSZ
31/6-1
Northern Horda Platform
Brage Horst
ØF (C)
Central Viking Graben
East Shetland Platform
ØF (S)
25/4-6S
25/5-7
26/4-1
ØSZ
Beryl Embayment
USZ
Stord Basin
HSZ
Utsira High
South Viking Graben
15/3-6
16/15-1
Augvald Graben
16/4-3
16/5-1
16/6-1
ÅF
Ling Depression
Åsta Graben
KSZ
Sele High
SSZ
Stavanger Platform
Witch Ground Graben
Norwegian-Danish Basin
NSDZ
Western Gneiss Region
BASZ
Bergen
Stavanger
Zechstein Salt limit

Figure 5

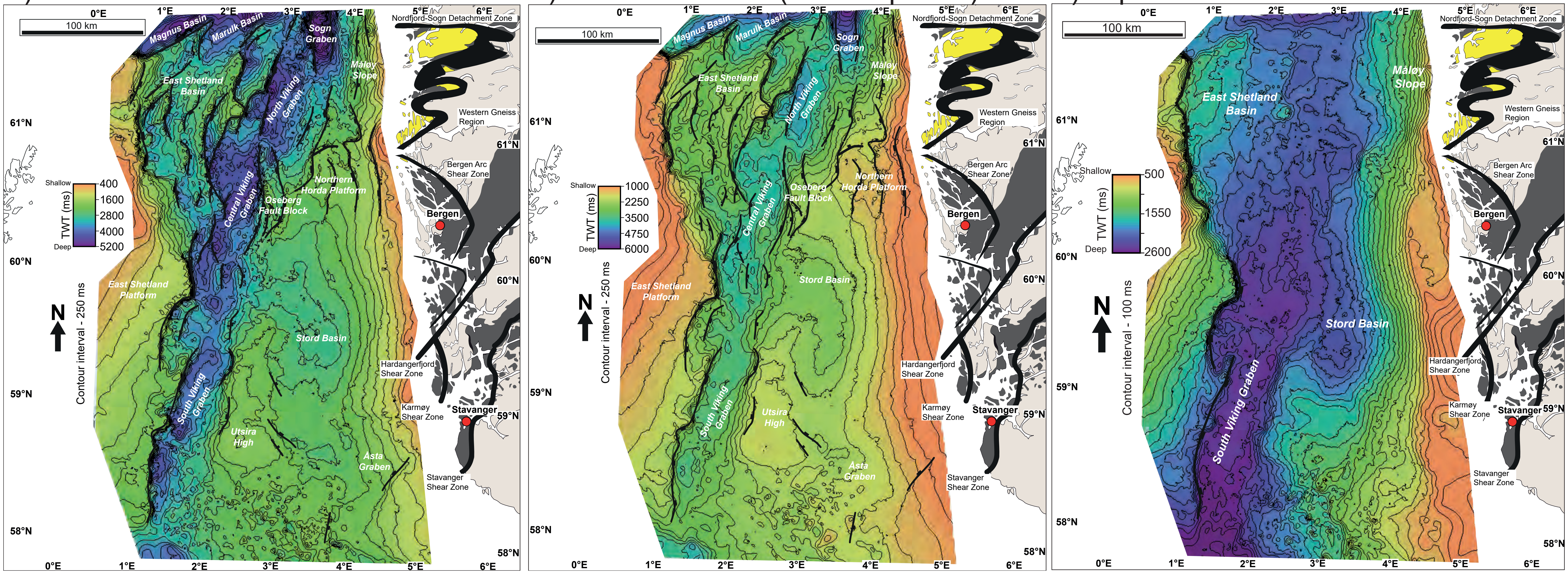
A) Middle Jurassic - Base RP2
B) Base Cret. Unc. (Near Top RP2)
C) Top Cretaceous - Post-rift
100 km
Magnus Basin
Marulk Basin
Sogn Graben
Måløy Slope
East Shetland Basin
North Viking Graben
Western Gneiss Region
Nordfjord-Sogn Detachment Zone
Bergen Arc Shear Zone
Bergen
Central Viking Graben
Oseberg Fault Block
Northern Horda Platform
East Shetland Platform
Stord Basin
Hardangerfjord Shear Zone
Karmøy Shear Zone
Stavanger
Stavanger Shear Zone
South Viking Graben
Utsira High
Asta Graben
Shallow
Deep
TWT (ms)
400
1600
2800
4000
5200
1000
2250
3500
4750
6000
500
1550
2600
Contour interval - 250 ms
Contour interval - 100 ms
N
0°E
1°E
2°E
3°E
4°E
5°E
6°E
58°N
59°N
60°N
61°N

Figure 6

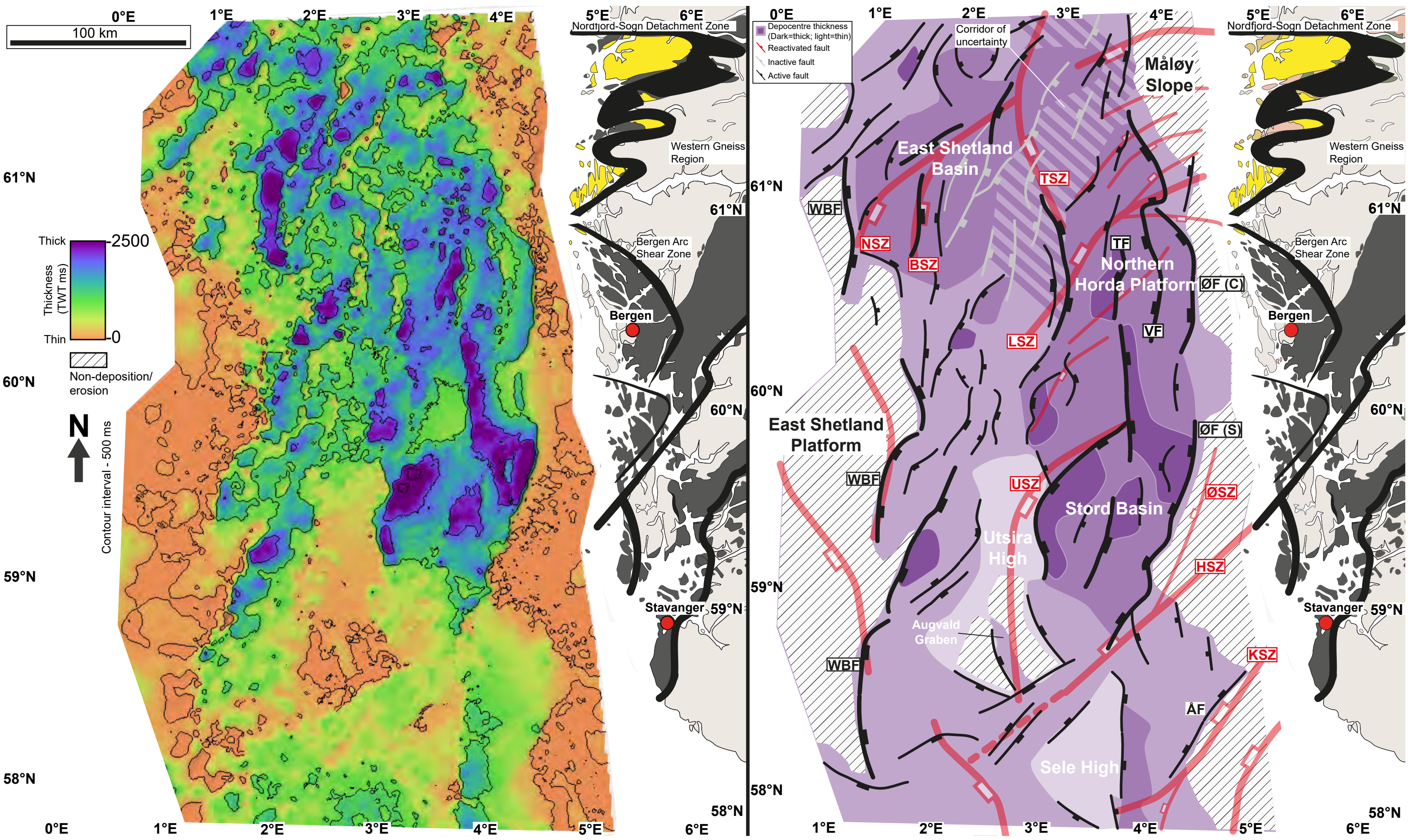

100 km
0°E
1°E
2°E
3°E
4°E
5°E
6°E
61°N
60°N
59°N
58°N
Thick
Thin
2500
0
Thickness (TWT ms)
Non-deposition/ erosion
N
Contour interval - 500 ms
Nordfjord-Sogn Detachment Zone
Western Gneiss Region
Bergen Arc Shear Zone
Bergen
Stavanger
Depocentre thickness (Dark=thick; light=thin)
Reactivated fault
Inactive fault
Active fault
Corridor of uncertainty
East Shetland Basin
Måløy Slope
TSZ
NSZ
BSZ
WBF
TF
Northern Horda Platform
ØF (C)
LSZ
VF
East Shetland Platform
ØF (S)
USZ
ØSZ
Stord Basin
Utsira High
HSZ
Augvald Graben
KSZ
AF
Sele High

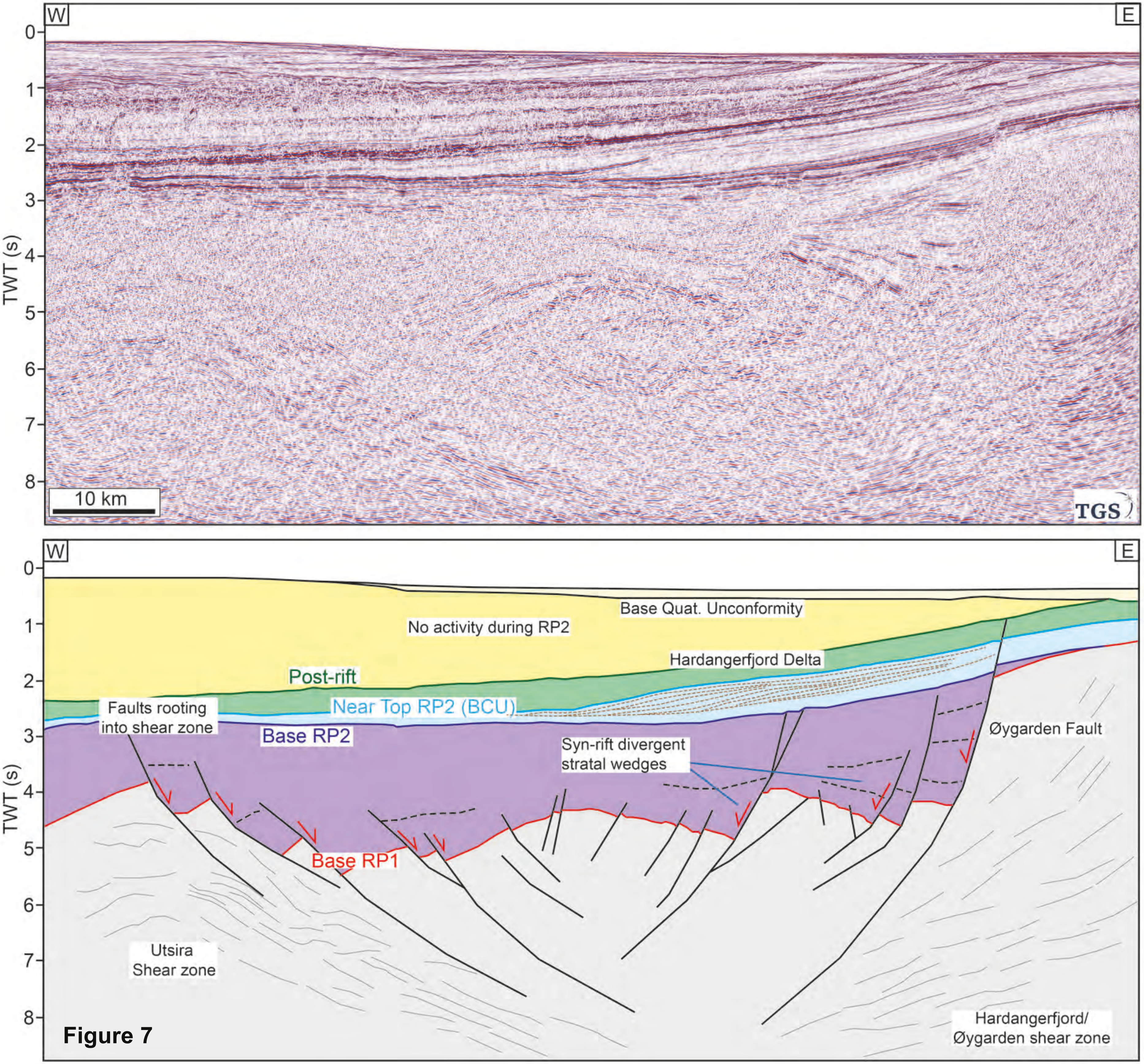

W
E
0
1
2
3
4
5
6
7
8
TWT (s)
10 km
TGS
W
E
TWT (s)
Base Quat. Unconformity
No activity during RP2
Hardangerfjord Delta
Post-rift
Faults rooting
into shear zone
Near Top RP2 (BCU)
Base RP2
Syn-rift divergent
stratal wedges
Øygarden Fault
Base RP1
Utsira
Shear zone
Hardangerfjord/
Øygarden shear zone

Figure 7

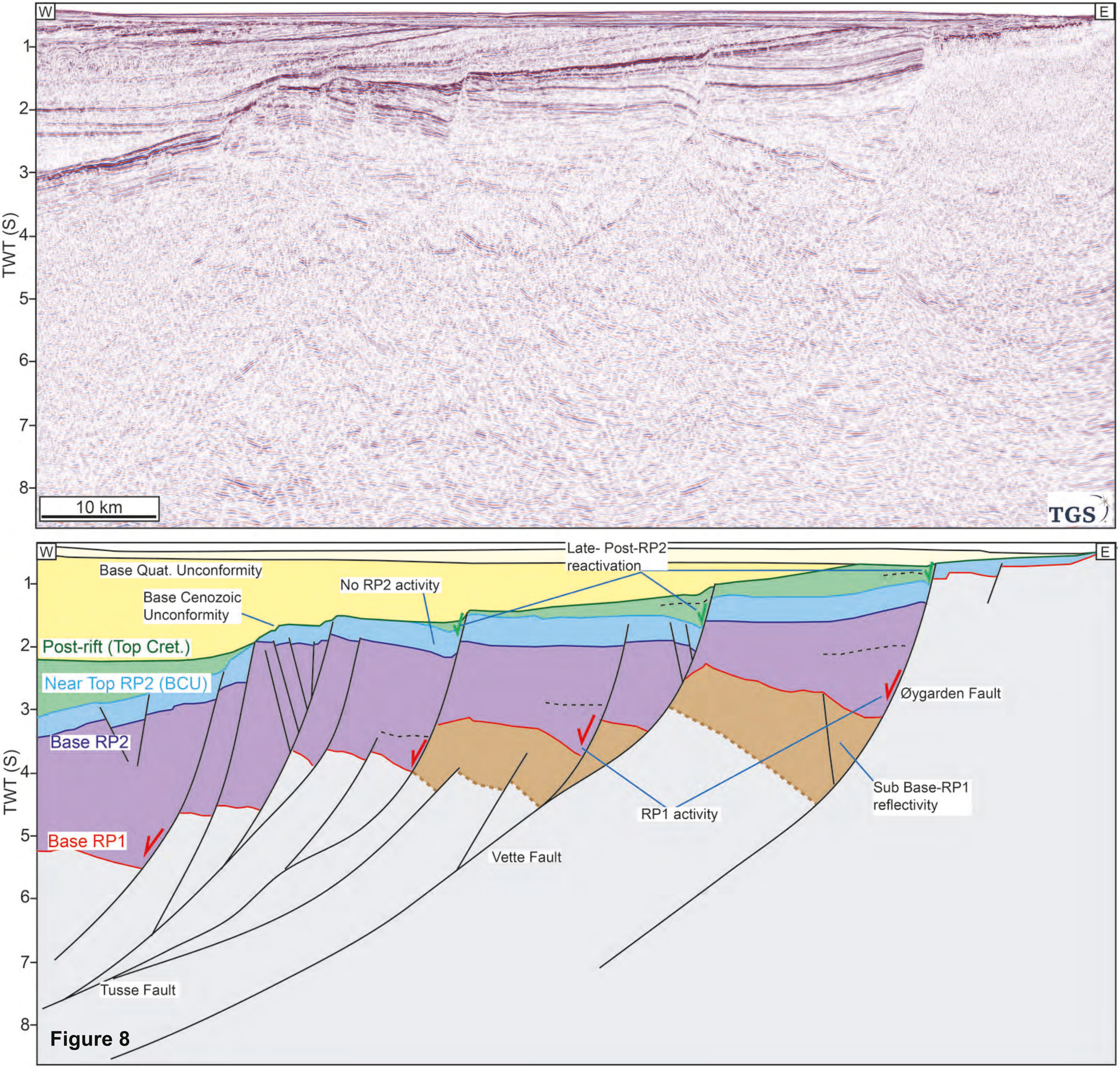

W
E
TWT (S)
10 km
TGS
Late- Post-RP2 reactivation
Base Quat. Unconformity
No RP2 activity
Base Cenozoic Unconformity
Post-rift (Top Cret.)
Near Top RP2 (BCU)
Base RP2
Base RP1
Øygarden Fault
RP1 activity
Sub Base-RP1 reflectivity
Vette Fault
Tusse Fault

Figure 8

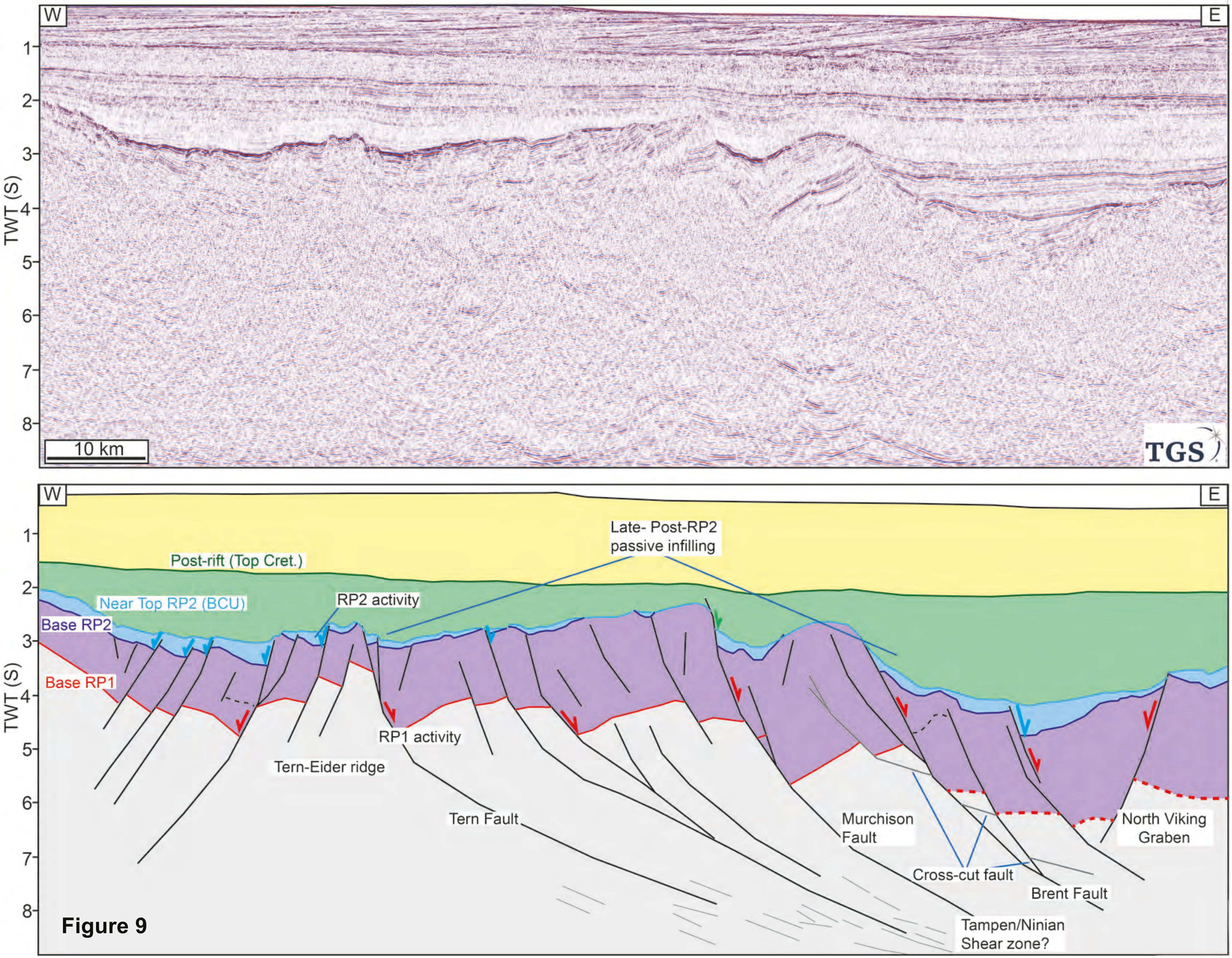
W
E
TWT (S)
1
2
3
4
5
6
7
8
10 km
TGS
Late- Post-RP2
passive infilling
Post-rift (Top Cret.)
Near Top RP2 (BCU)
RP2 activity
Base RP2
Base RP1
RP1 activity
Tern-Eider ridge
Tern Fault
Murchison
Fault
North Viking
Graben
Cross-cut fault
Brent Fault
Tampen/Ninian
Shear zone?
Figure 9

Figure 10

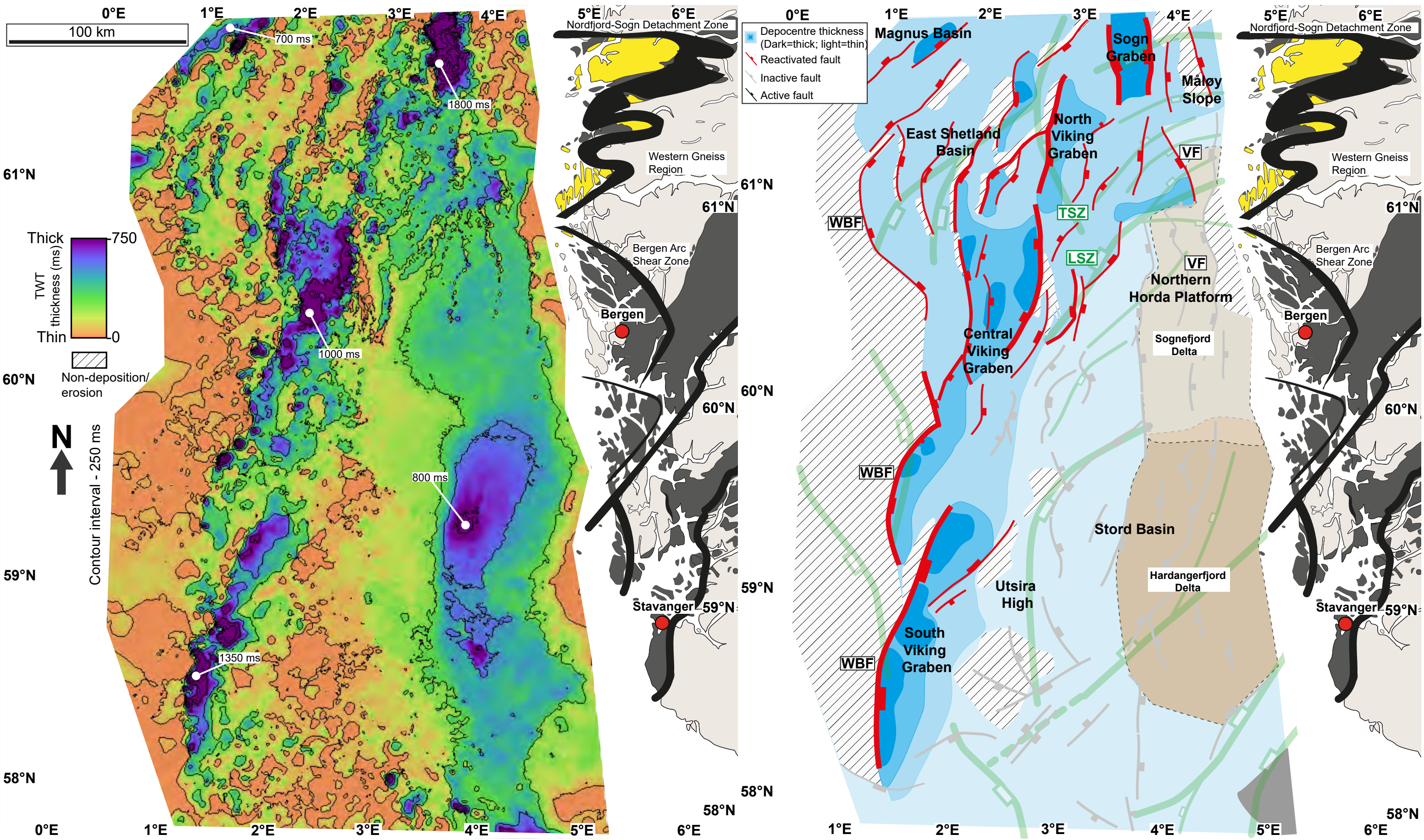

100 km
0°E
1°E
2°E
3°E
4°E
5°E
6°E
Nordfjord-Sogn Detachment Zone
700 ms
1800 ms
1000 ms
800 ms
1350 ms
Thick
Thin
750
0
TWT thickness (ms)
Non-deposition/ erosion
N
Contour interval - 250 ms
61°N
60°N
59°N
58°N
Western Gneiss Region
Bergen Arc Shear Zone
Bergen
Stavanger
Depocentre thickness (Dark=thick; light=thin)
Reactivated fault
Inactive fault
Active fault
Magnus Basin
Sogn Graben
Måløy Slope
East Shetland Basin
North Viking Graben
VF
TSZ
LSZ
WBF
Northern Horda Platform
Sognefjord Delta
Central Viking Graben
Stord Basin
Hardangerfjord Delta
Utsira High
South Viking Graben

Figure 11

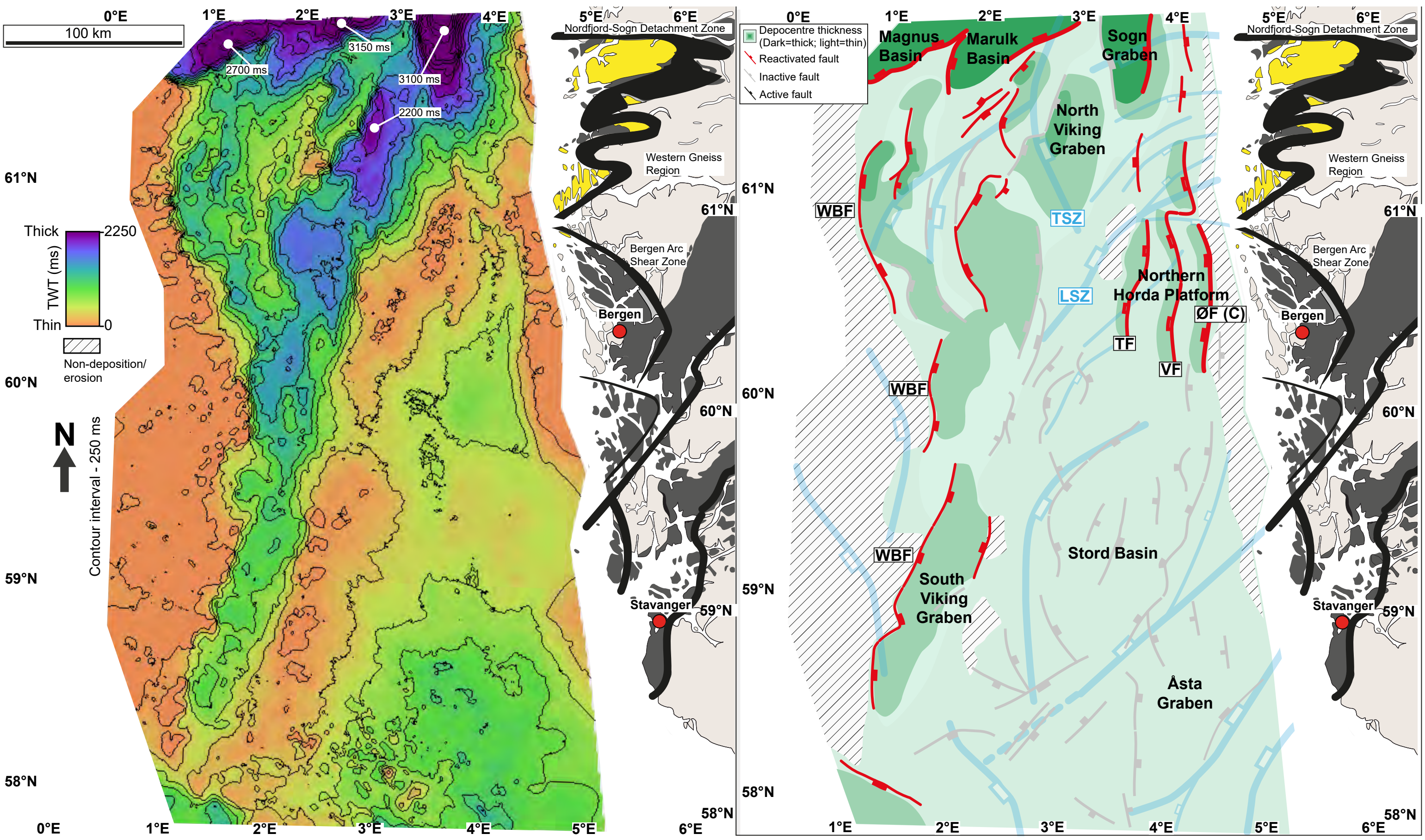

100 km
0°E
1°E
2°E
3°E
4°E
5°E
6°E
2700 ms
3150 ms
3100 ms
2200 ms
61°N
60°N
59°N
58°N
Thick
Thin
TWT (ms)
2250
0
Non-deposition/
erosion
N
Contour interval - 250 ms
Nordfjord-Sogn Detachment Zone
Western Gneiss
Region
Bergen Arc
Shear Zone
Bergen
Stavanger
Depocentre thickness
(Dark=thick; light=thin)
Reactivated fault
Inactive fault
Active fault
Magnus
Basin
Marulk
Basin
Sogn
Graben
North
Viking
Graben
WBF
TSZ
LSZ
Northern
Horda Platform
ØF (C)
TF
VF
Stord Basin
South
Viking
Graben
Åsta
Graben

Figure 12

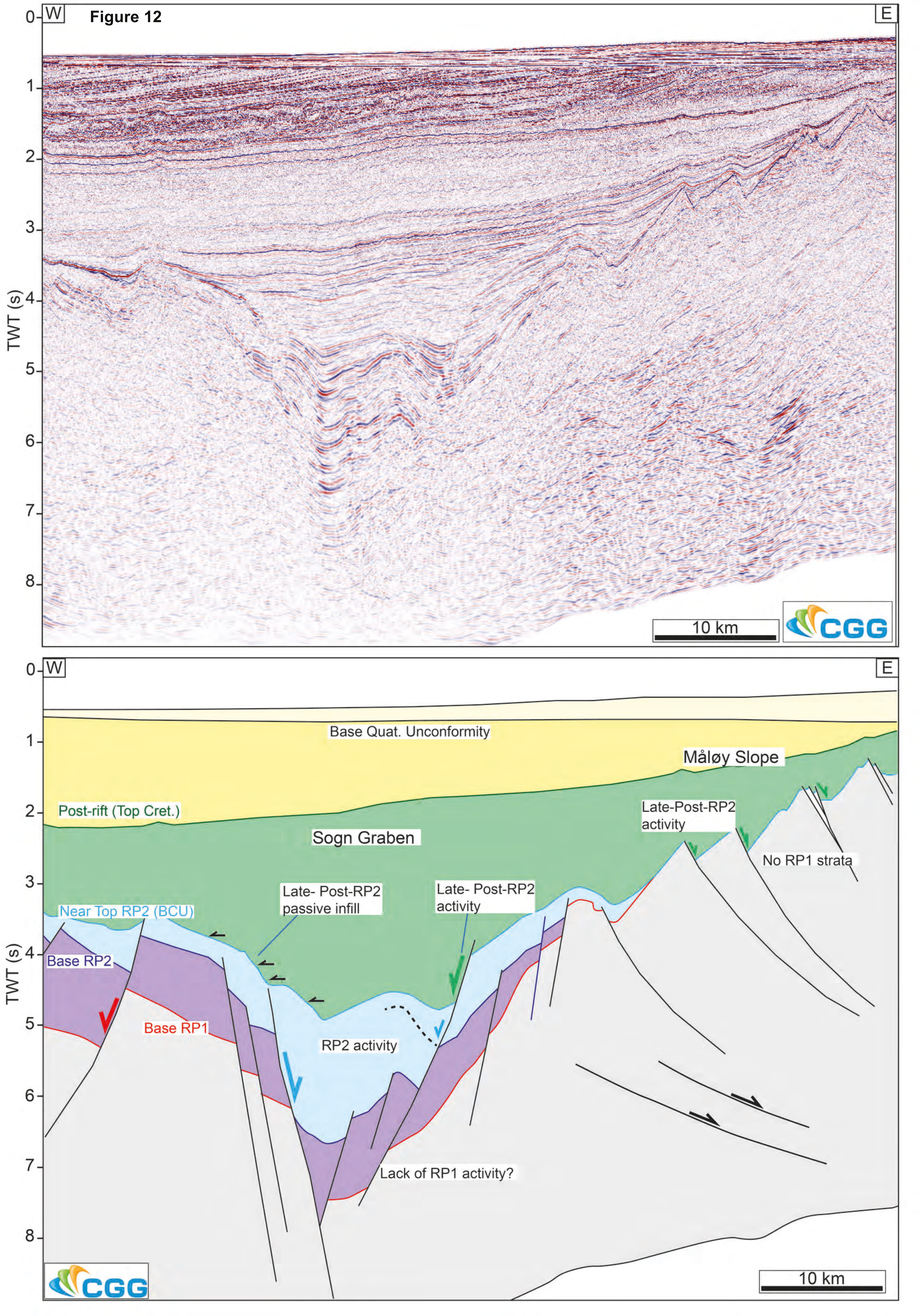
W
E
TWT (s)
0
1
2
3
4
5
6
7
8
10 km
CGG
Base Quat. Unconformity
Måløy Slope
Post-rift (Top Cret.)
Sogn Graben
Late-Post-RP2
activity
No RP1 strata
Late- Post-RP2
passive infill
Late- Post-RP2
activity
Near Top RP2 (BCU)
Base RP2
Base RP1
RP2 activity
Lack of RP1 activity?

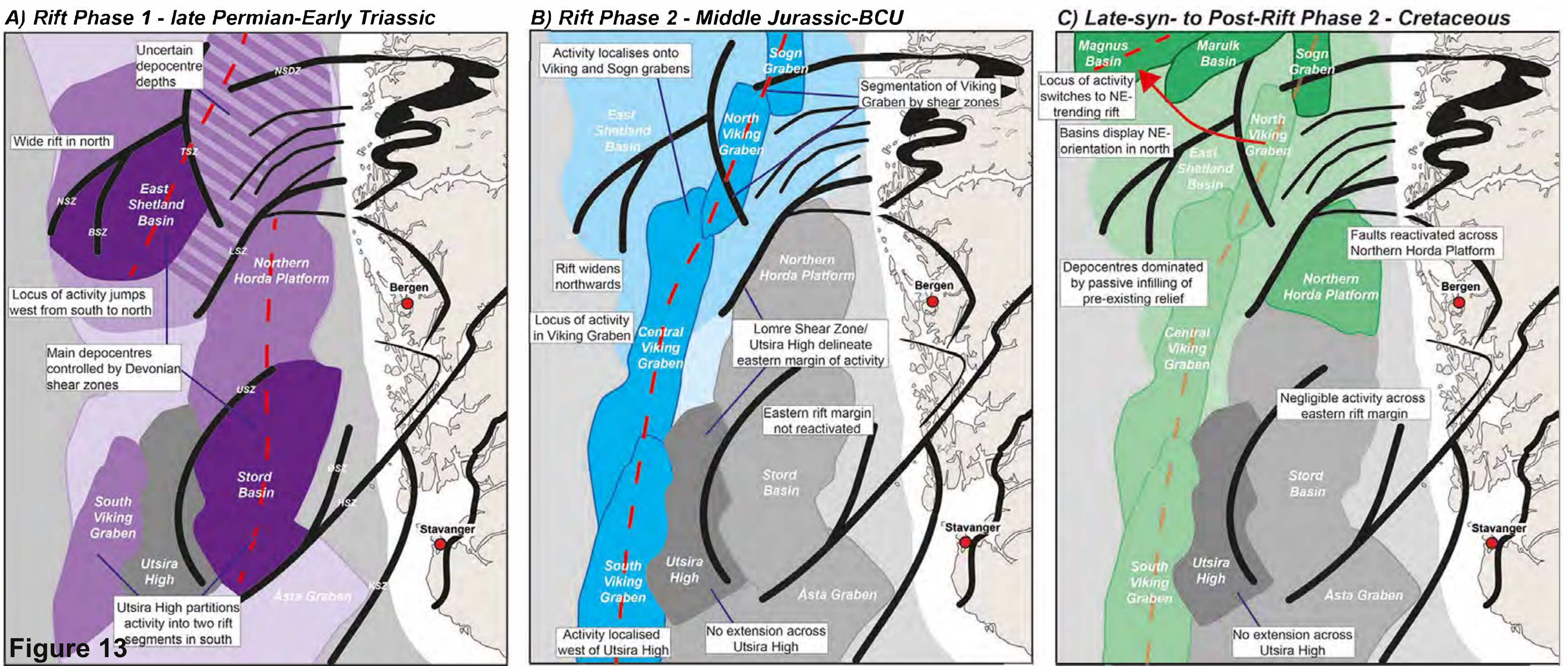
A) Rift Phase 1 - late Permian-Early Triassic
Uncertain depocentre depths
NSDZ
Wide rift in north
TSZ
NSZ
BSZ
East Shetland Basin
LSZ
Northern Horda Platform
Bergen
Locus of activity jumps west from south to north
Main depocentres controlled by Devonian shear zones
USZ
South Viking Graben
Utsira High
Stord Basin
ØSZ
HSZ
Stavanger
KSZ
Åsta Graben
Utsira High partitions activity into two rift segments in south
B) Rift Phase 2 - Middle Jurassic-BCU
Activity localises onto Viking and Sogn grabens
Sogn Graben
Segmentation of Viking Graben by shear zones
East Shetland Basin
North Viking Graben
Rift widens northwards
Northern Horda Platform
Bergen
Locus of activity in Viking Graben
Central Viking Graben
Lomre Shear Zone/ Utsira High delineate eastern margin of activity
Eastern rift margin not reactivated
Stord Basin
Stavanger
South Viking Graben
Utsira High
Åsta Graben
Activity localised west of Utsira High
No extension across Utsira High
C) Late-syn- to Post-Rift Phase 2 - Cretaceous
Magnus Basin
Marulk Basin
Sogn Graben
Locus of activity switches to NE-trending rift
North Viking Graben
Basins display NE-orientation in north
East Shetland Basin
Faults reactivated across Northern Horda Platform
Depocentres dominated by passive infilling of pre-existing relief
Northern Horda Platform
Bergen
Central Viking Graben
Negligible activity across eastern rift margin
Stord Basin
Stavanger
South Viking Graben
Utsira High
Åsta Graben
No extension across Utsira High

Figure 13

Figure 14

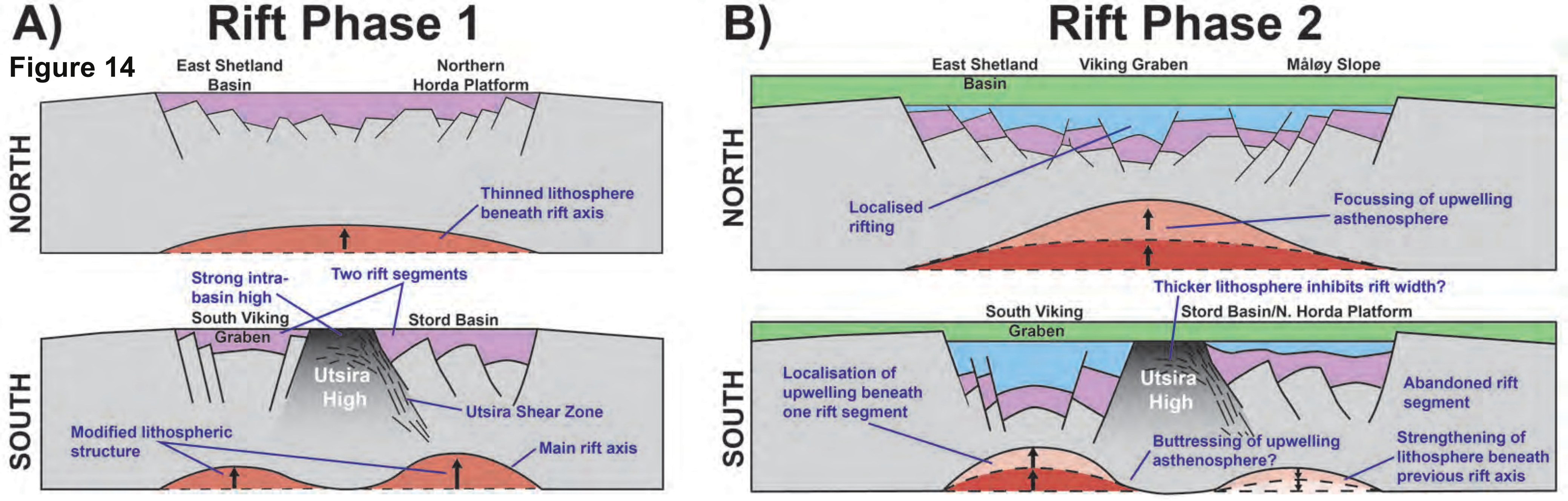

A)
Rift Phase 1
East Shetland
Basin
Northern
Horda Platform
NORTH
Thinned lithosphere
beneath rift axis
Strong intra-
basin high
Two rift segments
South Viking
Graben
Stord Basin
Utsira
High
Utsira Shear Zone
SOUTH
Modified lithospheric
structure
Main rift axis
B)
Rift Phase 2
East Shetland
Basin
Viking Graben
Måløy Slope
NORTH
Localised
rifting
Focussing of upwelling
asthenosphere
Thicker lithosphere inhibits rift width?
South Viking
Graben
Stord Basin/N. Horda Platform
Localisation of
upwelling beneath
one rift segment
Utsira
High
Abandoned rift
segment
SOUTH
Buttressing of upwelling
asthenosphere?
Strengthening of
lithosphere beneath
previous rift axis

Figure 15

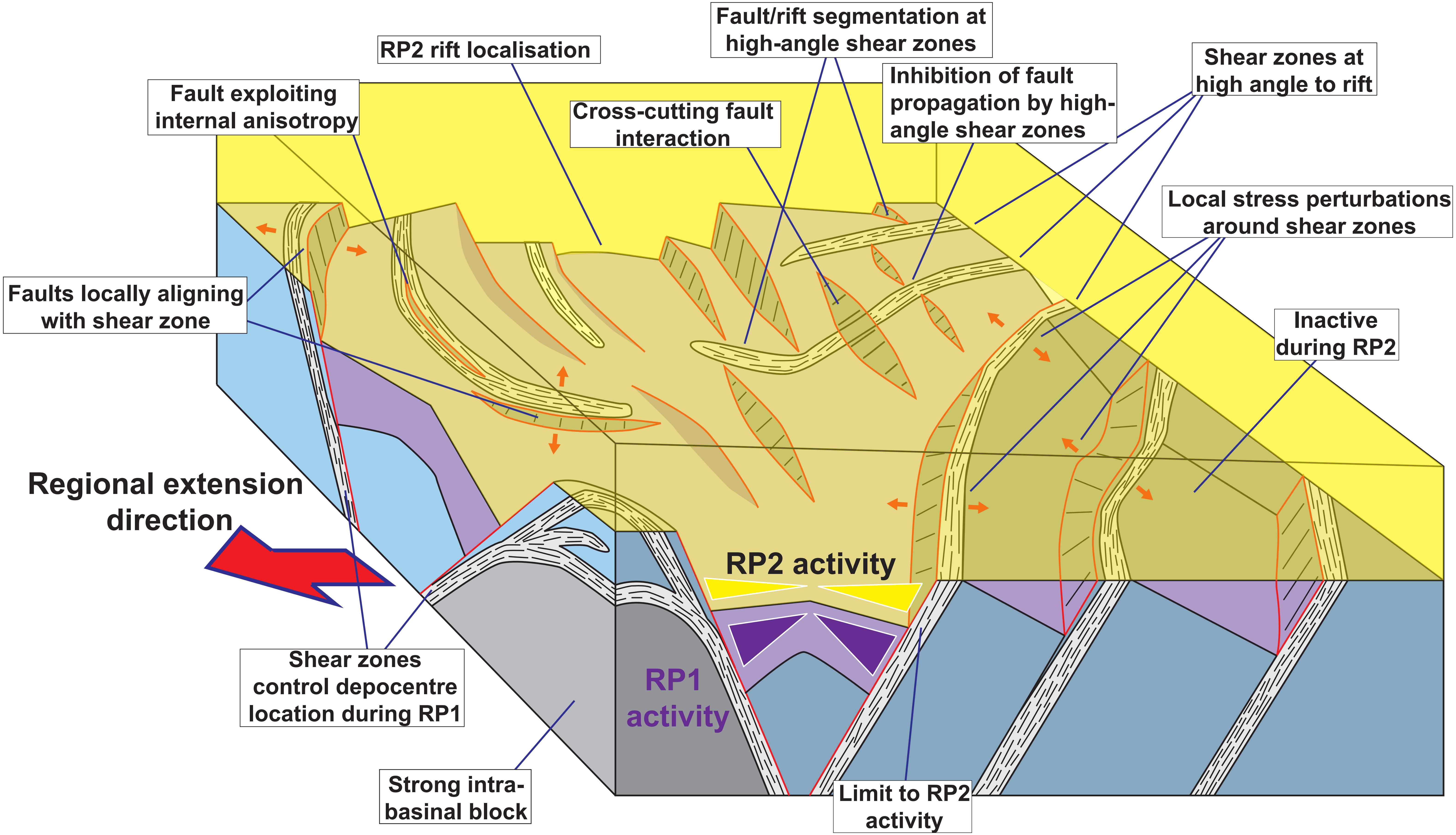

RP2 rift localisation
Fault/rift segmentation at high-angle shear zones
Fault exploiting internal anisotropy
Cross-cutting fault interaction
Inhibition of fault propagation by high-angle shear zones
Shear zones at high angle to rift
Local stress perturbations around shear zones
Faults locally aligning with shear zone
Inactive during RP2
Regional extension direction
RP2 activity
RP1 activity
Shear zones control depocentre location during RP1
Strong intra-basinal block
Limit to RP2 activity